

Air Force Institute of Technology

AFIT Scholar

Faculty Publications

4-7-2017

Periodic Traveling Interfacial Hydroelastic Waves with or without Mass

Benjamin F. Akers

Air Force Institute of Technology

David A. Ambrose

Drexel University

David W. Sulon

Drexel University

Follow this and additional works at: <https://scholar.afit.edu/facpub>



Part of the [Mathematics Commons](#)

Recommended Citation

Akers, B. F., Ambrose, D. M., & Sulon, D. W. (2017). Periodic traveling interfacial hydroelastic waves with or without mass. *Zeitschrift Für Angewandte Mathematik Und Physik*, 68(6), 141. <https://doi.org/10.1007/s00033-017-0884-7>

This Article is brought to you for free and open access by AFIT Scholar. It has been accepted for inclusion in Faculty Publications by an authorized administrator of AFIT Scholar. For more information, please contact richard.mansfield@afit.edu.

PERIODIC TRAVELING INTERFACIAL HYDROELASTIC WAVES WITH OR WITHOUT MASS

BENJAMIN F. AKERS, DAVID M. AMBROSE, AND DAVID W. SULON

ABSTRACT. We study the motion of an interface between two irrotational, incompressible fluids, with elastic bending forces present; this is the hydroelastic wave problem. We prove a global bifurcation theorem for the existence of families of spatially periodic traveling waves on infinite depth. Our traveling wave formulation uses a parameterized curve, in which the waves are able to have multi-valued height. This formulation and the presence of the elastic bending terms allows for the application of an abstract global bifurcation theorem of “identity plus compact” type. We furthermore perform numerical computations of these families of traveling waves, finding that, depending on the choice of parameters, the curves of traveling waves can either be unbounded, reconnect to trivial solutions, or end with a wave which has a self-intersection. Our analytical and computational methods are able to treat in a unified way the cases of positive or zero mass density along the sheet, the cases of single-valued or multi-valued height, and the cases of single-fluid or interfacial waves.

1. INTRODUCTION

We study the motion of an elastic, frictionless membrane of non-negative mass between two irrotational, incompressible fluids. This is known as a hydroelastic wave problem. Each fluid has its own non-negative density, and if one of these densities is equal to zero, this is the hydroelastic water wave case. Hydroelastic waves can occur in several scenarios, such as a layer of ice above the ocean [24] (for which the water wave case would be relevant), or a flapping flag in a fluid [7] (for which the interfacial case would be relevant).

To model the elastic effects at the free surface, we use the Cosserat theory of elastic shells as developed and described by Plotnikov and Toland [20]. This system is more suitable for large surface deformations than simpler models such as linear or Kirchoff-Love models. The second author, Siegel, and Liu have shown that the initial value problems for these Cosserat-type hydroelastic waves are well-posed in Sobolev spaces [8], [16]. Toland and Baldi and Toland have proved existence of periodic traveling hydroelastic water waves with and without mass including studying secondary bifurcations [25], [26], [10], [11]. A number of authors have also computed traveling hydroelastic water waves, finding results in 2D and 3D, computations of periodic and solitary waves, comparison with weakly nonlinear models, and comparison across different modelling assumptions for the bending force [13], [14], [17], [18], [19], [28], [29]. While we believe these computations of hydroelastic water waves are the most relevant such studies to the present work,

This work was supported in part from a grant from the Office of Naval Research (ONR grant APSHEL to Dr. Akers).

Dr. Ambrose is grateful to support from the NSF through grant DMS-1515849.

this is not an exhaustive list, and the interested reader is encouraged to consult these papers for further references.

We use the formulation for traveling waves introduced by two of the authors and Wright [2]. This version of the traveling wave ansatz is valid for a traveling parameterized curve, and thus extreme behavior of the waves, such as overturning, may be studied. Furthermore, while the present study concerns waves in two-dimensional fluids, the formulation based on a traveling parameterized curve extends to the case of a traveling parameterized surface in three space dimensions. Thus, this method of allowing for overturning waves generalizes to the higher-dimensional case, unlike methods based on complex analysis; this has been carried out in one case already [6].

In [2], the density-matched vortex sheet with surface tension was studied. The particular results in [2] are that the formulation for a traveling parameterized curve was introduced and was used to prove a local bifurcation theorem, and families of waves were computed, showing that curves of traveling waves typically ended when a self-intersecting wave was reached. Subsequently, Akers, Ambrose, and Wright showed that Crapper waves, a family of exact pure capillary traveling water waves, could be perturbed by including the effect of gravity, and the formulation was again used to compute these waves [5]. Further numerical results were demonstrated in [4], where the non-density-matched vortex sheet was considered. The formulation was also used to prove a global bifurcation theorem for vortex sheets with surface tension for arbitrary constant densities, and thus including the water wave case [9].

We give details of this formulation in Section 2 below, after first stating the evolution equations for the hydroelastic wave problem. While the evolution equations, and thus the traveling wave equations, are different in the cases with and without mass (i.e., the case of zero mass density or positive mass density along the elastic sheet), this difference goes away when applying the abstract global bifurcation theorem. This is because the terms involving the mass parameter are nonlinear, and vanish when linearizing about equilibrium. We are therefore able to treat the two cases simultaneously in the analysis.

The abstract bifurcation theorem we apply requires a one-dimensional kernel in our linearized operator. For certain values of the parameters, there may instead be a two-dimensional kernel. The authors will treat the cases of two-dimensional kernels in a subsequent paper. This will involve studying secondary bifurcations as in [10], and also studying Wilton ripples [22], [23], [30], [3], [27].

In Section 3 we state and prove our main theorem, which is a global bifurcation theorem for periodic traveling hydroelastic waves, giving several conditions for how a curve of such waves might end. In Section 4, we describe our numerical method for computing curves of traveling waves, and we give numerical results.

2. GOVERNING EQUATIONS

2.1. Equations of motion. The setup of our problem closely mirrors that of [9] and [16]. We consider two two-dimensional fluids, each of which may possess a different mass density. A one-dimensional interface I (a free surface) comprises the boundary between these two fluid regions; one fluid (with density $\rho_1 \geq 0$) lies below I , while the other (with density $\rho_2 \geq 0$) lies above I . The fluid regions are infinite in the vertical direction, and are periodic in the horizontal direction. In our model, we allow the interface itself to possess non-negative mass density ρ . Our model also

includes the effects of hydroelasticity and surface tension on the interface; these will be presented later in this section as we introduce the full equations of motion.

Within the interior of each fluid region, the fluid's velocity u is governed by the irrotational, incompressible Euler equations:

$$\begin{aligned} u_t + u \cdot \nabla u &= -\nabla p, \\ \operatorname{div}(u) &= 0, \\ u &= \nabla \phi; \end{aligned}$$

however, since u may jump across I , there is may still be measure-valued vorticity whose support is I . We can write this vorticity in the form $\gamma \delta_I$, where $\gamma \in \mathbb{R}$ (which may vary along I) is called the “unnormalized vortex sheet-strength,” and δ_I is the Dirac mass of I [9].

Identifying our overall region with \mathbb{C} , we parametrize I as a curve $z(\alpha, t) = x(\alpha, t) + iy(\alpha, t)$ with periodicity conditions

$$\begin{aligned} (1a) \quad x(\alpha + 2\pi, t) &= x(\alpha, t) + M, \\ (1b) \quad y(\alpha + 2\pi, t) &= y(\alpha, t), \end{aligned}$$

for some $M > 0$ (throughout, α will be our spatial parameter along the interface, and t will represent time). Let U and V denote the normal and tangential velocities, respectively; i.e.

$$(2) \quad z_t = UN + VT,$$

where

$$\begin{aligned} T &= \frac{z_\alpha}{s_\alpha}, \\ N &= i \frac{z_\alpha}{s_\alpha}, \\ (3) \quad s_\alpha^2 &= |z_\alpha|^2 = x_\alpha^2 + y_\alpha^2. \end{aligned}$$

(Notice that T and N are the complex versions of the unit tangent and upward normal vectors to the curve.) We choose a normalized arclength parametrization; i.e. we enforce

$$(4) \quad s_\alpha = \sigma(t) := \frac{L(t)}{2\pi}$$

at all times t , where $L(t)$ is the length of one period of the interface. Thus, in our parametrization, s_α is constant with respect to α . Furthermore, we define the tangent angle

$$\theta = \arctan\left(\frac{y_\alpha}{x_\alpha}\right);$$

it is clear that the curve z can be constructed (up to one point) from information about θ and σ , and that curvature of the interface κ can be given as

$$\kappa = \frac{\theta_\alpha}{s_\alpha}.$$

The normal velocity U (a geometric invariant) is determined entirely by the Birkhoff-Rott integral:

$$(5) \quad U = \operatorname{Re}(W^*N),$$

where

$$(6) \quad W^*(\alpha, t) = \frac{1}{2\pi i} \text{PV} \int_{\mathbb{R}} \frac{\gamma(\alpha', t)}{z(\alpha, t) - z(\alpha', t)} d\alpha'.$$

We are free to choose the tangential velocity V in order to enforce our parametrization (4). Explicitly, we choose periodic V such that

$$(7) \quad V_\alpha = \theta_\alpha U - \frac{1}{2\pi} \int_0^{2\pi} \theta_\alpha U d\alpha.$$

We can differentiate both sides of (3) by t , and obtain

$$s_{\alpha t} = V_\alpha - \theta_\alpha U;$$

using this and (7), we can then write

$$(8) \quad s_{\alpha t} = -\frac{1}{2\pi} \int_0^{2\pi} \theta_\alpha U d\alpha = \frac{1}{2\pi} \int_0^{2\pi} (s_{\alpha t} - V_\alpha) d\alpha = \frac{1}{2\pi} \int_0^{2\pi} s_{\alpha t} d\alpha.$$

Note that the last step is justified since V is periodic. But, we also have

$$L = \int_0^{2\pi} s_\alpha d\alpha,$$

so (8) reduces to

$$s_{\alpha t} = \frac{L_t}{2\pi},$$

which yields (4) for all times t as long as (4) holds at $t = 0$.

The evolution of the interface is also determined by the behavior of the vortex sheet-strength $\gamma(\alpha, t)$, which can be written in terms of the jump in tangential velocity across the surface. Using a model which combines those used in [8] and [16], we assume the jump in pressure across the interface to be

$$[[p]] = \rho(\text{Re}(W_t^* N) + V_W \theta_t) + \frac{1}{2} E_b \left(\kappa_{ss} + \frac{\kappa^3}{2} - \tau_1 \kappa \right) + g \rho \text{Im} N,$$

where $\rho \geq 0$ is the mass density of the interface, $V_W := V - \text{Re}(W^* T)$, $E_b \geq 0$ is the bending modulus, $\tau_1 > 0$ is a surface tension parameter, and g is acceleration due to gravity. Then, we can write an equation for γ_t [16]:

$$(9) \quad \begin{aligned} \gamma_t &= -\frac{\tilde{S}}{\sigma^3} \left(\partial_\alpha^4 \theta + \frac{3\theta_\alpha^2 \theta_{\alpha\alpha}}{2} - \tau_1 \sigma^2 \theta_{\alpha\alpha} \right) + \frac{(V_W \gamma)_\alpha}{\sigma} - 2\tilde{A}(\text{Re}(W_{\alpha t}^* N)) \\ &\quad - \left(2A - \frac{2\tilde{A}\theta_\alpha}{\sigma} \right) (\text{Re}(W_t^* T)) s_\alpha - 2\tilde{A} \left((V_W)_\alpha \theta_t + V_W \theta_{t\alpha} + \frac{g x_{\alpha\alpha}}{\sigma} \right) \\ &\quad - 2A \left(\frac{\gamma \gamma_\alpha}{4\sigma^2} - V_W \text{Re}(W_\alpha^* T) + g y_\alpha \right). \end{aligned}$$

In addition to those defined above, equation (9) includes the following constant quantities; some are listed with their physical meanings:

$$\begin{aligned} \rho_1 & : \text{ density of the lower fluid } (\geq 0), \\ \rho_2 & : \text{ density of the upper fluid } (\geq 0), \\ \tilde{S} & := \frac{E_b}{\rho_1 + \rho_2} (\geq 0), \\ A & := \frac{\rho_1 - \rho_2}{\rho_1 + \rho_2} \text{ (the "Atwood number," } \in [-1, 1]), \\ \tilde{A} & := \frac{\rho}{\rho_1 + \rho_2} (\geq 0). \end{aligned}$$

We can nondimensionalize, and write (9) in the form

$$\begin{aligned} (10) \quad \gamma_t & = -\frac{S}{\sigma^3} \left(\partial_\alpha^4 \theta + \frac{3\theta_\alpha^2 \theta_{\alpha\alpha}}{2} - \tau_1 \sigma^2 \theta_{\alpha\alpha} \right) + \frac{(V_W \gamma)_\alpha}{\sigma} \\ & \quad - 2\tilde{A} (\text{Re}(W_{\alpha t}^* N)) - \left(2A - \frac{2\tilde{A}\theta_\alpha}{\sigma} \right) (\text{Re}(W_t^* T)) s_\alpha \\ & \quad - 2\tilde{A} \left((V_W)_\alpha \theta_t + V_W \theta_{t\alpha} + \frac{x_{\alpha\alpha}}{\sigma} \right) - 2A \left(\frac{\gamma\gamma_\alpha}{4\sigma^2} - V_W \text{Re}(W_\alpha^* T) + y_\alpha \right), \end{aligned}$$

where $S = \tilde{S} / |g|$. In the two-dimensional hydroelastic vortex sheet problem with mass, the interface's motion is thus governed by (2), (5), (6), (7), and (10).

2.2. Traveling wave ansatz. We wish to consider traveling wave solutions to the two-dimensional hydroelastic vortex sheet problem with mass.

Definition 1. *Suppose (z, γ) is a solution to (2), (5), (6), (7), and (10) that additionally satisfies $(z, \gamma)_t = (c, 0)$ for some real parameter c . We then say (z, γ) is a traveling wave solution to (2), (5), (6), (7), and (10) with speed c .*

Remark 2. *In our application of global bifurcation theory to show existence of traveling wave solutions, the value c will serve as our bifurcation parameter.*

Note that under the traveling wave assumption, we clearly have

$$\begin{aligned} U & = -c \sin \theta, \\ V & = c \cos \theta. \end{aligned}$$

By carefully differentiating under the integral (in the principal value sense), it can be shown that under the traveling wave assumption, both $W_t^* = 0$ and $W_{\alpha t}^* = 0$. Thus, both terms $2\tilde{A} (\text{Re}(W_{\alpha t}^* N))$ and $\left(2A - \frac{2\tilde{A}\theta_\alpha}{\sigma} \right) (\text{Re}(W_t^* T)) s_\alpha$ vanish in the traveling wave case, and (10) reduces to

$$\begin{aligned} 0 & = -\frac{S}{\sigma^3} \left(\partial_\alpha^4 \theta + \frac{3\theta_\alpha^2 \theta_{\alpha\alpha}}{2} - \tau_1 \sigma^2 \theta_{\alpha\alpha} \right) + \frac{(V_W \gamma)_\alpha}{\sigma} \\ & \quad - 2\tilde{A} \left((V_W)_\alpha \theta_t + V_W \theta_{t\alpha} + \frac{x_{\alpha\alpha}}{\sigma} \right) - 2A \left(\frac{\gamma\gamma_\alpha}{4\sigma^2} - V_W \text{Re}(W_\alpha^* T) + y_\alpha \right), \end{aligned}$$

or

$$\begin{aligned} (11) \quad 0 & = -\frac{S}{\sigma^3} \left(\partial_\alpha^4 \theta + \frac{3\theta_\alpha^2 \theta_{\alpha\alpha}}{2} - \tau_1 \sigma^2 \theta_{\alpha\alpha} \right) + \frac{(V_W \gamma)_\alpha}{\sigma} \\ & \quad - 2\tilde{A} \partial_\alpha \left(V_W \theta_t + \frac{x_\alpha}{\sigma} \right) - 2A \left(\frac{\gamma\gamma_\alpha}{4\sigma^2} - V_W \text{Re}(W_\alpha^* T) + y_\alpha \right). \end{aligned}$$

Note that

$$V_W = V - \operatorname{Re}(W^*T) = c \cos \theta - \operatorname{Re}(W^*T),$$

and

$$\begin{aligned} y_\alpha &= \sigma \sin \theta, \\ x_\alpha &= \sigma \cos \theta; \end{aligned}$$

also, θ_t clearly vanishes in the traveling wave case. We also have

$$(c \cos \theta - \operatorname{Re}(W^*T)) (\operatorname{Re}(W_\alpha^*T)) = -\frac{1}{2} \partial_\alpha \left\{ (c \cos \theta - \operatorname{Re}(W^*T))^2 \right\},$$

which is shown in [9], or could be computed from the above. Thus, we can substitute the above, and write (11) as

$$(12) \quad 0 = -\frac{S}{\sigma^3} \left(\partial_\alpha^4 \theta + \frac{3\theta_\alpha^2 \theta_{\alpha\alpha}}{2} - \tau_1 \sigma^2 \theta_{\alpha\alpha} \right) - 2\tilde{A} (\cos \theta)_\alpha \\ + \frac{((c \cos \theta - \operatorname{Re}(W^*T)) \gamma)_\alpha}{\sigma} - A \left(\frac{\partial_\alpha (\gamma^2)}{4\sigma^2} + 2\sigma \sin \theta + \partial_\alpha \left\{ (c \cos \theta - \operatorname{Re}(W^*T))^2 \right\} \right).$$

We multiply both sides by σ/τ_1 :

$$(13) \quad 0 = -\frac{S}{\tau_1 \sigma^2} \left(\partial_\alpha^4 \theta + \frac{3\theta_\alpha^2 \theta_{\alpha\alpha}}{2} - \tau_1 \sigma^2 \theta_{\alpha\alpha} \right) - \frac{2\tilde{A}\sigma}{\tau_1} (\cos \theta)_\alpha \\ + \frac{1}{\tau_1} ((c \cos \theta - \operatorname{Re}(W^*T)) \gamma)_\alpha \\ - \frac{A}{\tau_1} \left(\frac{\partial_\alpha (\gamma^2)}{4\sigma} + 2\sigma^2 \sin \theta + \sigma \partial_\alpha \left\{ (c \cos \theta - \operatorname{Re}(W^*T))^2 \right\} \right).$$

For concision, we define

$$(14) \quad \Phi(\theta, \gamma; c, \sigma) := \frac{1}{\tau_1} ((c \cos \theta - \operatorname{Re}(W^*T)) \gamma)_\alpha \\ - \frac{A}{\tau_1} \left[\frac{(\gamma^2)_\alpha}{4\sigma} + 2\sigma^2 \sin \theta + \sigma \partial_\alpha \left\{ (c \cos \theta - \operatorname{Re}(W^*T))^2 \right\} \right].$$

(We define Φ in this manner so that it corresponds with the mapping Φ defined in [9]; there, this mapping comprises all of the lower-order terms.) Then, (13) can be written as

$$0 = -\frac{S}{\tau_1 \sigma^2} \left(\partial_\alpha^4 \theta + \frac{3\theta_\alpha^2 \theta_{\alpha\alpha}}{2} - \tau_1 \sigma^2 \theta_{\alpha\alpha} \right) - \frac{2\tilde{A}\sigma}{\tau_1} (\cos \theta)_\alpha + \Phi(\theta, \gamma; c, \sigma),$$

or

$$(15) \quad 0 = \partial_\alpha^4 \theta + \frac{3\theta_\alpha^2 \theta_{\alpha\alpha}}{2} - \tau_1 \sigma^2 \theta_{\alpha\alpha} + \frac{2\tilde{A}\sigma^3}{S} (\cos \theta)_\alpha - \frac{\tau_1 \sigma^2}{S} \Phi(\theta, \gamma; c, \sigma).$$

We label the remaining lower-order terms as

$$\begin{aligned} \Psi_1(\theta; \sigma) &:= \frac{3}{2} \theta_\alpha^2 \theta_{\alpha\alpha}, \\ \Psi_2(\theta; \sigma) &:= -\tau_1 \sigma^2 \theta_{\alpha\alpha}, \\ \Psi_3(\theta; \sigma) &:= \frac{2\tilde{A}\sigma^3}{S} (\cos \theta)_\alpha; \end{aligned}$$

note that Ψ_3 is the only remaining term that includes the effect of interface mass. Combining these together as $\Psi := \Psi_1 + \Psi_2 + \Psi_3$, we write (15) as

$$(16) \quad 0 = \partial_\alpha^4 \theta + \Psi(\theta; \sigma) - \frac{\tau_1 \sigma^2}{S} \Phi(\theta, \gamma; c, \sigma).$$

Recall that (5) also determines the behavior of the interface. Since $U = -c \sin \theta$, (5) becomes (as in [9])

$$(17) \quad 0 = \operatorname{Re}(W^* N) + c \cos \theta.$$

Note that (16) and (17) feature z and θ interchangeably. From this point onward, we would like to look for traveling wave solutions in the form (θ, γ) alone; thus, it becomes important to explicitly state how to construct z from θ (in a unique manner, up to rigid translation) in the traveling wave case. We can clearly do this via

$$(18) \quad z(\alpha, 0) = z(\alpha, t) - ct = \sigma \int_0^\alpha \exp(i\theta(\alpha')) \, d\alpha'.$$

Then, given the work completed throughout this section thus far, it is clear that if $(\theta, \gamma; c)$ satisfy (16) and (17) (with z appearing in $\operatorname{Re}(W^* N)$ constructed from θ via 18), then (z, γ) is a traveling wave solution to (2), (5) and (10) with speed c (again, with z constructed via (18)).

It is as this point, however, that we arrive at a technical issue. Even if $(\theta, \gamma; c)$ yield a traveling wave solution (z, γ) , we cannot expect that 2π -periodic θ to yield periodic z via (18). We would like for any 2π -periodic (θ, γ) that solve some equations analogous to (16) and (17) to correspond directly to a *periodic* traveling wave solution (z, γ) of (2), (5), and (10). Hence, in a manner closely analogous to [9], we modify the mappings in (16) and (17) to ensure this.

2.3. Periodicity considerations. Throughout this section, assume that θ is a sufficiently smooth, 2π -periodic function. Define the following mean quantities:

$$\overline{\cos \theta} := \frac{1}{2\pi} \int_0^{2\pi} \cos(\theta(\alpha')) \, d\alpha', \quad \overline{\sin \theta} := \frac{1}{2\pi} \int_0^{2\pi} \sin(\theta(\alpha')) \, d\alpha'.$$

Given $M > 0$ and θ with $\overline{\cos \theta} \neq 0$, define the “renormalized curve”

$$\tilde{Z}[\theta](\alpha) := \frac{M}{2\pi \overline{\cos \theta}} \left[\int_0^\alpha \exp(i\theta(\alpha')) \, d\alpha' - i\alpha \overline{\sin \theta} \right].$$

Note that $\tilde{Z}[\theta]$ is one derivative smoother than θ , and a direct calculation shows that such a curve in fact satisfies our original spacial periodicity requirement (1a), (1b):

$$\tilde{Z}[\theta](\alpha + 2\pi) = \tilde{Z}[\theta](\alpha) + M.$$

Also, we clearly have normal and tangent vectors to $\tilde{Z}[\theta]$ given by

$$\begin{aligned} \tilde{T}[\theta] &= \frac{\partial_\alpha \tilde{Z}[\theta]}{|\partial_\alpha \tilde{Z}[\theta]|}, \\ \tilde{N}[\theta] &= i \frac{\partial_\alpha \tilde{Z}[\theta]}{|\partial_\alpha \tilde{Z}[\theta]|}. \end{aligned}$$

Next, we use a specific form of the Birkhoff-Rott integral (for real-valued γ and complex-valued ω that satisfy $\omega(\alpha + 2\pi) = \omega(\alpha) + M$):

$$B[\omega]\gamma(\alpha) := \frac{1}{2iM} \text{PV} \int_{\mathbb{R}} \gamma(\alpha') \cot\left(\frac{\pi}{M}(\omega(\alpha) - \omega(\alpha'))\right) d\alpha'.$$

As discussed in [9], setting $\omega = z$ yields $W^* = B[z]\gamma$, where W^* is as defined in (6); this follows from the well-known cotangent series expansion due to Mittag-Leffler (which can, for example, be found in [1]). We are now ready to define a mapping $\tilde{\Phi}$, analogous to the mapping in [9]:

$$\begin{aligned} \tilde{\Phi}(\theta, \gamma; c) &:= \frac{1}{\tau_1} \partial_\alpha \left\{ c \cos \theta - \text{Re} \left(\left(B[\tilde{Z}[\theta]]\gamma \right) \tilde{T}[\theta] \right) \gamma \right\} \\ &\quad - \frac{A}{\tau_1} \left(\frac{\pi \overline{\cos \theta}}{2M} \partial_\alpha(\gamma^2) + \frac{M^2}{2\pi^2 (\cos \theta)^2} (\sin \theta - \overline{\sin \theta}) \right) \\ &\quad - \frac{A}{\tau_1} \left(\frac{M}{2\pi \cos \theta} \partial_\alpha \left\{ \left(c \cos \theta - \text{Re} \left(\left(B[\tilde{Z}[\theta]]\gamma \right) \tilde{T}[\theta] \right) \right)^2 \right\} \right). \end{aligned}$$

This construction is enough for us to ensure M -periodicity in a traveling-wave wave solution to (16) and (17):

Proposition 3. *Suppose $c \neq 0$ and 2π -periodic functions θ, γ satisfy $\overline{\cos \theta} \neq 0$ and*

$$(19) \quad \text{Re} \left(\left(B[\tilde{Z}[\theta]]\gamma \right) \tilde{N}[\theta] \right) + c \sin \theta = 0,$$

$$(20) \quad \partial_\alpha^4 \theta + \Psi(\theta; \sigma) - \frac{\tau_1 \sigma^2}{S} \tilde{\Phi}(\theta, \gamma; c) = 0,$$

with $\sigma = M/(2\pi \overline{\cos \theta})$. Then, $(\tilde{Z}[\theta](\alpha) + ct, \gamma(\alpha))$ is a traveling wave solution to (16) and (17) with speed c , and $\tilde{Z}[\theta](\alpha) + ct$ is spatially periodic with period M .

A proof of a proposition almost identical to Proposition 3 can be found in [9]. Under the assumptions of this proposition, we can see how (19) corresponds to (17) given our construction above; then, [9] shows that (under these assumptions) $\tilde{\Phi}(\theta, \gamma; c) = \Phi(\theta, \gamma; c, \sigma)$ with $\sigma = M/(2\pi \overline{\cos \theta})$.

We thus will henceforth work with equations (19), (20), though a few more steps are needed in order to bring these equations into a form conducive to applying the global bifurcation theory.

2.4. Final reformulation. We wish to “solve” (20) for θ . To do so, we introduce an inverse derivative operator ∂_α^{-4} , which we define in Fourier space. For a general 2π -periodic map μ with convergent Fourier series, let $\hat{\mu}(k)$ denote the k^{th} Fourier coefficient in the usual sense, i.e. $\mu(\alpha) = \sum_{k=-\infty}^{\infty} \hat{\mu}(k) \exp(ik\alpha)$. Then, define for μ with mean zero (i.e. $\hat{\mu}(0) = 0$)

$$(21) \quad \begin{cases} \widehat{\partial_\alpha^{-4} \mu}(k) := k^{-4} \hat{\mu}(k), & k \neq 0 \\ \widehat{\partial_\alpha^{-4} \mu}(0) := 0. \end{cases}$$

By this construction, ∂_α^{-4} clearly preserves periodicity, and for sufficiently regular, periodic μ with mean zero,

$$\partial_\alpha^{-4} \partial_\alpha^4 \mu = \mu = \partial_\alpha^4 \partial_\alpha^{-4} \mu.$$

Also, define the projection P (here, μ may not necessarily have mean zero):

$$(22) \quad P\mu(\alpha) := \mu(\alpha) - \frac{1}{2\pi} \int_0^{2\pi} \mu(\alpha') d\alpha';$$

it is clear that $P\mu$ has mean zero. We apply $\partial_\alpha^{-4}P$ to both sides of (20), and obtain the equation

$$(23) \quad 0 = \theta + \partial_\alpha^{-4}P\Psi(\theta; \sigma) - \frac{\tau_1\sigma^2}{S} \partial_\alpha^{-4}P\tilde{\Phi}(\theta, \gamma; c)$$

(throughout, note $\sigma = M/(2\pi\overline{\cos\theta})$).

Next, we approach (19). First, we subtract the mean $\bar{\gamma} := (2\pi)^{-1} \int_0^{2\pi} \gamma(\alpha) d\alpha$ from γ and write

$$\gamma_1 := \gamma - \bar{\gamma},$$

As in [9], the Birkhoff-Rott integral can be decomposed as

$$(24) \quad B[\omega]\gamma(\alpha) = \frac{1}{2i\omega_\alpha(\alpha)} H\gamma(\alpha) + \mathcal{K}[\omega]\gamma(\alpha),$$

where the most singular portion

$$(25) \quad H\gamma(\alpha) := \frac{1}{2\pi} \text{PV} \int_0^{2\pi} \gamma(\alpha') \cot\left(\frac{1}{2}(\alpha - \alpha')\right) d\alpha'$$

is the Hilbert transform, and the remainder

$$\mathcal{K}[\omega]\gamma(\alpha) := \frac{1}{4\pi i} \text{PV} \int_0^{2\pi} \gamma(\alpha') \left[\cot\left(\frac{1}{2}(\omega(\alpha) - \omega(\alpha'))\right) - \frac{1}{\partial_{\alpha'}\omega(\alpha')} \cot\left(\frac{1}{2}(\alpha - \alpha')\right) \right] d\alpha'$$

is smooth on the domain we later define in Section 3.2.2. Then, as is also done in [9], we write (19) in the form

$$(26) \quad \gamma_1 - H\left\{2\left|\partial_\alpha\tilde{Z}[\theta]\right|\text{Re}\left(\left(\mathcal{K}[\tilde{Z}[\theta]](\bar{\gamma} + \gamma_1)\right)\tilde{N}[\theta]\right) + 2c\left|\partial_\alpha\tilde{Z}[\theta]\right|\sin\theta\right\} = 0.$$

Define

$$\Theta(\theta, \gamma_1; c) := \frac{\tau_1\sigma^2}{S} \partial_\alpha^{-4}P\tilde{\Phi}(\theta, \gamma_1 + \bar{\gamma}; c) - \partial_\alpha^{-4}P\Psi(\theta; \sigma),$$

so (23) becomes

$$(27) \quad \theta - \Theta(\theta, \gamma_1; c) = 0.$$

We then substitute $\theta = \Theta(\theta, \gamma_1; c)$ into (26) to obtain

$$(28) \quad \gamma_1 - \Gamma(\theta, \gamma_1; c) = 0,$$

where

$$(29) \quad \Gamma(\theta, \gamma_1; c) := H\left\{2\left|\partial_\alpha\tilde{Z}[\Theta(\theta, \gamma_1; c)]\right|\text{Re}\left(\left(\mathcal{K}[\tilde{Z}[\Theta(\theta, \gamma_1; c)]](\bar{\gamma} + \gamma_1)\right)\tilde{N}[\Theta(\theta, \gamma_1; c)]\right) + 2c\left|\partial_\alpha\tilde{Z}[\Theta(\theta, \gamma_1; c)]\right|\sin(\Theta(\theta, \gamma_1; c))\right\}.$$

In Section 3.2.2, we will show compactness of (Θ, Γ) given appropriate choice of domain, as the bifurcation theorem we shall apply to (27), (28) requires an ‘‘identity plus compact’’ formulation.

3. GLOBAL BIFURCATION THEOREM

3.1. Main theorem. We now present a global bifurcation theorem for the traveling wave problem. In essence, this theorem shows the existence of a rich variety of nontrivial solution sets. We prove this theorem throughout this section.

Theorem 4. *Let all be as defined in the previous section. For all choices of constants $M > 0$, $S > 0$, $\tau_1 > 0$, $A \in [-1, 1]$, $\tilde{A} \geq 0$, $\bar{\gamma} \in \mathbb{R}$, there exists a countable number of connected sets of smooth, non-trivial traveling-wave solutions of the two-dimensional hydroelastic vortex sheet problem with mass (i.e. solutions to $(\theta - \Theta(\theta, \gamma_1; c), \gamma_1 - \Gamma(\theta, \gamma_1; c)) = (0, 0; c)$). If $\bar{\gamma} \neq 0$ or $A \neq 0$, then each of these connected sets have at least one of the following properties (a) – (e):*

- (a): *It contains waves with arbitrarily long interface lengths per period*
- (b): *It contains waves whose interfaces have curvature with arbitrarily large derivative*
- (c): *It contains waves in which the derivative of the jump of the tangential component of fluid velocity can be arbitrarily large*
- (d): *Its closure contains a wave whose interface self-intersects*
- (e): *It contains a sequence of waves whose interface converge to a trivial solution but whose speeds contain at least two convergent subsequences whose limits differ.*

If $\bar{\gamma} = 0$ and $A = 0$, then another possible outcome is

- (f): *It contains waves which have speeds which are arbitrarily large.*

Remark 5. *The possible outcomes listed in the above theorem are very similar to the analogous main theorem of [9]. Notably different is outcome (b), where we list the possibility for the derivative of curvature to arbitrarily grow (instead of merely curvature itself). This distinction arises from a difference in domain spaces used; here, we require θ to possess one higher derivative than in [9].*

3.2. Global bifurcation results.

3.2.1. General global bifurcation theory. Our main theorem posits the existence of certain solution sets to the traveling wave problem; we show that this essentially follows directly from an application of a global bifurcation theorem due to Rabinowitz [21] and generalized by Kielhöfer [15]. The conditions of the theorem require a notion of *odd crossing number* for families of bounded linear operators.

Definition 6. *Assume $A(c)$ is a family of bounded linear operators depending continuously on a real parameter c . Suppose at some $c = c_0$, $A(c)$ has a zero eigenvalue. Define $\sigma^<(c) := 1$ if there are no negative real eigenvalues of $A(c)$ that perturb from this zero eigenvalue of $A(c_0)$, and $\sigma^<(c) := (-1)^{m_1 + \dots + m_k}$ if μ_1, \dots, μ_k are all negative real eigenvalues of $A(c)$ that perturb from this zero eigenvalue of $A(c_0)$, each with algebraic multiplicities m_1, \dots, m_k . We say $A(c)$ has an odd crossing number at $c = c_0$ if (i) $A(c)$ is regular for $c \in (c_0 - \delta, c_0) \cup (c_0, c_0 + \delta)$ and (ii) $\sigma^<(c)$ changes sign at $c = c_0$.*

Remark 7. *We can think of the crossing number itself as the number of real eigenvalues (counted with algebraic multiplicity) of $A(c)$ that pass through 0 as c moves across c_0 [9].*

We now state the abstract theorem as it appears in [9], which itself is a slight modification of the Kielhöfer version (see Remark 9 below).

Theorem 8. *(General bifurcation theorem). Let X be a Banach space, and let U be an open subset of $X \times \mathbb{R}$. Let F map U continuously into X . Assume that*

- (a): *the Frechet derivative $D_\xi F(0, \cdot)$ belongs to $C(\mathbb{R}, L(X, X))$*
- (b): *the mapping $(\xi, c) \mapsto F(\xi, c) - \xi$ is compact from $X \times \mathbb{R}$ into X , and*
- (c): *$F(0, c_0) = 0$ and $D_x F(0, c)$ has an odd crossing number at $c = c_0$.*

Let S denote the closure of the set of nontrivial solutions of $F(\xi, c) = 0$ in $X \times \mathbb{R}$. Let C denote the connected component of S to which $(0, c_0)$ belongs. Then, one of the following alternatives is valid:

- (i): *C is unbounded; or*
- (ii): *C contains a point $(0, c_1)$ where $c_0 \neq c_1$; or*
- (iii): *C contains a point on the boundary of U .*

Remark 9. *The Kielhöfer version of the theorem explicitly assumes the case $U = X \times \mathbb{R}$. The proof, however, is easily modified to admit general open $U \subseteq X \times \mathbb{R}$. The choice of such U for our problem will ensure well-definedness and compactness of our mapping (Θ, Γ) .*

One condition for Theorem 8 is that the mapping in question can be written in the form “identity plus compact.” We show that (Θ, Γ) is in fact compact over an appropriately chosen domain.

3.2.2. *Mapping properties.* To begin, we set up the necessary notation for the function spaces we wish to work with.

Definition 10. *Let H_{per}^s denote $H_{per}^s[0, 2\pi]$, i.e. the usual Sobolev space of 2π -periodic functions from \mathbb{R} to \mathbb{C} with square-integrable derivatives up to order $s \in \mathbb{N}$. Let $H_{per, odd}^s$ denote the subset of H_{per}^s comprised of odd functions; define $H_{per, even}^s$ similarly. Let $H_{per, 0, even}^s$ denote the subset of $H_{per, even}^s$ comprised of mean-zero functions. Finally, letting H_{loc}^s denote the usual Sobolev space of functions in $H^s(I)$ for all bounded intervals I , we put*

$$H_M^s = \left\{ \omega \in H_{loc}^s : \omega(\alpha) - \frac{M\alpha}{2\pi} \in H_{per}^s \right\}.$$

For $b \geq 0$ and $s \geq 2$, define the “chord-arc space”

$$C_b^s = \left\{ \omega \in H_M^s : \inf_{\alpha, \alpha' \in [a, b]} \left| \frac{\omega(\alpha) - \omega(\alpha')}{\alpha' - \alpha} \right| > b \right\}.$$

We are now ready to set an appropriate domain for (Θ, Γ) , and assert its compactness as a mapping over such domain.

Proposition 11. *Put*

$$X = H_{per,odd}^2 \times H_{per,0,even}^1 \times \mathbb{R}$$

and

$$(30) \quad U_{b,h} = \left\{ (\theta, \gamma_1; c) \in X : \overline{\cos \theta} > h, \tilde{Z}[\theta] \in C_b^2 \text{ and } \tilde{Z}[\Theta(\theta, \gamma_1; c)] \in C_b^5 \right\}.$$

The mapping (Θ, Γ) (where Θ, Γ are as defined in Section 2.4) from $U_{b,h} \subseteq X$ into X is compact.

Proof. The chord-arc conditions are imposed to ensure the well-definedness of the Birkhoff-Rott integral; this is seen in [9]. With these conditions, alongside the condition $\overline{\cos \theta} > h$, we ensure that each component of $\tilde{\Phi}$ is well-defined over $U_{b,h}$. It is also demonstrated in [9] that $\tilde{\Phi}$ costs a derivative in θ and retains derivatives in γ ; here, we have that $\tilde{\Phi}$ maps from $U_{b,h}$ to $H_{per,0}^1$. We need to check the mapping properties of Ψ (i.e., the terms that differ from the analogous equation of [9]). Recall that $\Psi := \Psi_1 + \Psi_2 + \Psi_3$, where

$$\begin{aligned} \Psi_1(\theta; \sigma) &= \frac{3}{2} \theta_\alpha^2 \theta_{\alpha\alpha} = \frac{1}{2} \partial_\alpha [\theta_\alpha^3] \\ \Psi_2(\theta; \sigma) &= -\tau_1 \sigma^2 \theta_{\alpha\alpha} \\ \Psi_3(\theta; \sigma) &= \frac{2\tilde{A}\sigma^3}{S} (\cos \theta)_\alpha \end{aligned}$$

Using elementary results regarding algebra properties for Sobolev spaces, we have that the maps $(\cdot)^3$ and $\cos(\cdot)$ both map from H_{per}^s to H_{per}^s as long as $s > \frac{n}{2} = \frac{1}{2}$. The choice $s = 2$ satisfies this. Also, if θ is odd, θ_α is even (as is θ_α^3), so $\partial_\alpha [\theta_\alpha^3]$ is odd. The function $\theta_{\alpha\alpha}$ is also odd, so Ψ_1, Ψ_2 maps into an “odd” space. Moreover, since $\partial_\alpha \cos(\theta) = -(\sin \theta) (\partial_\alpha \theta)$ and $\partial_\alpha \theta$ is even, we see that Ψ_3 maps into an “odd” space as well. Thus, we can write

$$\Psi : H_{per,odd}^2 \rightarrow H_{per,odd}^0,$$

so $\partial_\alpha^{-4} P\Psi$ maps into H_{per}^4 .

Furthermore, Ψ maps bounded sets to bounded sets as well, as each ∂_α is a bounded linear map between appropriate Sobolev spaces, and $(\cdot)^3$ also maps bounded sets to bounded sets given that its domain satisfies the condition $s > \frac{1}{2}$. Since ∂_α^{-4} and P are also bounded linear maps, we have that $\partial_\alpha^{-4} P\Psi$ maps bounded sets to bounded sets. Also, it is clear that $\partial_\alpha^{-4} P\Psi(\theta; \sigma)$ retains parity of θ .

We summarize the mapping properties as follows:

$$\begin{aligned} \tilde{\Phi} &: U_{b,h} \rightarrow H_{per,0,odd}^1, \\ \partial_\alpha^{-4} P\tilde{\Phi} &: U_{b,h} \rightarrow H_{per,odd}^5, \\ \partial_\alpha^{-4} P\Psi &: U_{b,h} \rightarrow H_{per,odd}^4, \end{aligned}$$

so by the above, we have by our definition of Θ ,

$$\Theta : U_{b,h} \rightarrow H_{per,odd}^4.$$

As in [9], Γ is written as a composition of Θ and an operator that neither gains nor costs derivatives, so

$$\Gamma : U_{b,h} \rightarrow H_{per,0,even}^4.$$

By Rellich's theorem, bounded sets in $H_{\text{per,odd}}^4$ are precompact in $H_{\text{per,odd}}^2$, and bounded sets $H_{\text{per,0,even}}^4$ are precompact in $H_{\text{per,0,even}}^1$. Each term of (Θ, Γ) maps bounded sets to bounded sets. Thus, by viewing (Θ, Γ) as a map from open $U_{b,h} \subseteq X$ into X , we have that (Θ, Γ) is a compact map. ■

We next compute the Frechét derivative of $(\theta - \Theta(\theta, \gamma_1; c), \gamma_1 - \Gamma(\theta, \gamma_1; c))$, and subsequently use this to analyze the crossing number.

3.2.3. Linearization calculation. In order to abbreviate the linearization calculations of (Θ, Γ) , we introduce some notation. For any map $\mu(\theta, \gamma_1; c)$, let $(\vec{\theta}, \vec{\gamma})$ denote the direction of differentiation, and define for general, sufficiently regular mappings μ

$$\begin{aligned} \mu_0 &:= \mu(0, 0; c) \\ D\mu &:= D_{\theta, \gamma_1} \mu(\theta, \gamma_1; c)|_{(0,0;c)} (\vec{\theta}, \vec{\gamma}) := \lim_{\varepsilon \rightarrow 0} \frac{1}{\varepsilon} \left(\mu(\varepsilon \vec{\theta}, \varepsilon \vec{\gamma}; c) - \mu_0 \right). \end{aligned}$$

Note that σ is dependent on θ ; we denote $\Sigma(\theta) := \sigma = M / (2\pi \overline{\cos \theta})$. We note the following elementary results:

$$\begin{aligned} \sin_0 &= 0, & D \cos &= 0 \\ \Sigma_0 &= \frac{M}{2\pi}, & D\Sigma &= 0. \end{aligned}$$

A large number of components of $(D\Theta, D\Gamma)$ were explicitly computed in [9]. Namely, these results yield for our closely analogous $\tilde{\Phi}$

$$D\tilde{\Phi} = -\frac{\pi\bar{\gamma}}{M} \left(-\frac{\bar{\gamma}}{\tau_1} + \frac{cAM}{\pi\tau_1} \right) \partial_\alpha H \vec{\theta} - \frac{AM^2}{2\pi^2\tau_1} P \vec{\theta} + \left(\frac{c}{\tau_1} - \frac{\pi A\bar{\gamma}}{\tau_1 M} \right) \partial_\alpha \vec{\gamma},$$

where the projection P is as defined in (22) and H is the Hilbert transform (see (25)). We need to compute the linearization of the ‘‘extra’’ terms Ψ_1, Ψ_2, Ψ_3 that (loosely) correspond to the hydroelastic and interface mass effects. Examine

$$\begin{aligned} D\Psi_1 &= \frac{1}{2} \partial_\alpha D [\theta_\alpha^3] \\ &= \frac{3}{2} \partial_\alpha [(\partial_\alpha \theta)^2 \partial_\alpha \vec{\theta}], \end{aligned}$$

so at $\theta = 0$, we see $D\Psi_1 = 0$. Next, we examine

$$\begin{aligned} D\Psi_2 &= D [-\tau_1 \Sigma^2 \partial_\alpha^2 \theta] \\ &= -\tau_1 (2\Sigma_0 D\Sigma [\partial_\alpha^2 \theta]_{\theta=0} + \Sigma_0^2 \partial_\alpha^2 D\theta) \\ &= -\tau_1 \left(0 + \left(\frac{M}{2\pi} \right)^2 \partial_\alpha^2 \vec{\theta} \right) \\ &= -\tau_1 \left(\frac{M}{2\pi} \right)^2 \partial_\alpha^2 \vec{\theta}, \end{aligned}$$

and

$$\begin{aligned}
D\Psi_3 &= D \left[-\frac{2\tilde{A}g\Sigma^3}{S} \sin(\theta) \theta_\alpha \right] \\
&= -\frac{2\tilde{A}}{S} \left[D(\Sigma^3) \sin_0 [\partial_\alpha(\theta)]_{\theta=0} + \Sigma_0^3 D \cos [\partial_\alpha(\theta)]_{\theta=0} + \Sigma_0^3 \sin_0 \partial_\alpha \vec{\theta} \right] \\
&= -\frac{2\tilde{A}}{S} [0 + 0 + 0] \\
&= 0.
\end{aligned}$$

Thus,

$$D\Psi = -\tau_1 \left(\frac{M}{2\pi} \right)^2 \partial_\alpha^2 \vec{\theta}.$$

We pause to remark that the crossing number is entirely determined by the linearization near equilibrium. Note that $D\Psi_3 = 0$ means that the presence of interface mass will not have any bearing on the application of Theorem 8 to our problem; in other words, the same conclusions about bifurcation (given odd crossing number) can be drawn in the $\tilde{A} = 0$ as in the $\tilde{A} > 0$ case.

Continuing, we recall the definition of Θ , and calculate

$$\begin{aligned}
D\Theta &= \partial_\alpha^{-4} P \left[\frac{\tau_1}{S} D(\Sigma^2 \tilde{\Phi}) - D\Psi \right] \\
&= \partial_\alpha^{-4} P \left[\frac{\tau_1}{S} (2\Sigma_0 D\Sigma \tilde{\Phi}_0 + \Sigma_0^2 D\tilde{\Phi}) - D\Psi \right] \\
&= \partial_\alpha^{-4} P \left[\frac{\tau_1}{S} \left(\frac{M}{2\pi} \right)^2 D\tilde{\Phi} - D\Psi \right] \\
&= \frac{\tau_1 \bar{\gamma} M}{4\pi S} \left(\frac{\bar{\gamma}}{\tau_1} - \frac{cAM}{\pi \tau_1} \right) \partial_\alpha^{-4} \partial_\alpha H \vec{\theta} - \frac{AM^4}{8\pi^4 S} \partial_\alpha^{-4} P \vec{\theta} + \frac{\tau_1 M^2}{4\pi^2} \partial_\alpha^{-4} \partial_\alpha^2 \vec{\theta} \\
&\quad - \frac{\tau_1 M^2}{4\pi^2 S} \left(\frac{\pi A \bar{\gamma}}{\tau_1 M} - \frac{c}{\tau_1} \right) \partial_\alpha^{-4} \partial_\alpha \vec{\gamma}.
\end{aligned}$$

The mapping Γ defined in (29) is the composition of Θ and a mapping identical to that which appears in [9]. It is shown in [9] that $D\Gamma = \frac{cM}{\pi} HD\Theta$, so by substituting our expression for $D\Theta$, we obtain

$$\begin{aligned}
D\Gamma &= \frac{c\tau_1 \bar{\gamma} M^2}{4\pi^2 S} \left(\frac{\bar{\gamma}}{\tau_1} - \frac{cAM}{\pi \tau_1} \right) H \partial_\alpha^{-4} \partial_\alpha H \vec{\theta} - \frac{cAM^5}{8\pi^5 S} H \partial_\alpha^{-4} P \vec{\theta} \\
&\quad + \frac{c\tau_1 M^3}{4\pi^3} H \partial_\alpha^{-4} \partial_\alpha^2 \vec{\theta} - \frac{c\tau_1 M^3}{4\pi^3 S} \left(\frac{\pi A \bar{\gamma}}{\tau_1 M} - \frac{c}{\tau_1} \right) H \partial_\alpha^{-4} \partial_\alpha \vec{\gamma}.
\end{aligned}$$

Combining our results for $D\Theta$, $D\Gamma$, we write the linearization L_c at $(0, 0; c)$ in matrix form:

$$(31) \quad L_c \begin{bmatrix} \vec{\theta} \\ \vec{\gamma} \end{bmatrix} := \begin{bmatrix} \vec{\theta} - D\Theta \\ \vec{\gamma} - D\Gamma \end{bmatrix},$$

where

$$L_c := \begin{bmatrix} L_{11} & L_{12} \\ L_{21} & L_{22} \end{bmatrix} \begin{bmatrix} \vec{\theta} \\ \vec{\gamma} \end{bmatrix},$$

with

$$\begin{aligned}
L_{11} &:= 1 - \frac{\tau_1 \bar{\gamma} M}{4\pi S} \left(\frac{\bar{\gamma}}{\tau_1} - \frac{cAM}{\pi \tau_1} \right) \partial_\alpha^{-4} \partial_\alpha H + \frac{AM^4}{8\pi^4 S} \partial_\alpha^{-4} P - \frac{\tau_1 M^2}{4\pi^2} \partial_\alpha^{-4} \partial_\alpha^2, \\
L_{12} &:= \frac{\tau_1 M^2}{4\pi^2 S} \left(\frac{\pi A \bar{\gamma}}{\tau_1 M} - \frac{c}{\tau_1} \right) \partial_\alpha^{-4} \partial_\alpha, \\
L_{21} &:= -\frac{c\tau_1 \bar{\gamma} M^2}{4\pi^2 S} \left(\frac{\bar{\gamma}}{\tau_1} - \frac{cAM}{\pi \tau_1} \right) H \partial_\alpha^{-4} \partial_\alpha H + \frac{cAM^5}{8\pi^5 S} H \partial_\alpha^{-4} P - \frac{c\tau_1 M^3}{4\pi^3} H \partial_\alpha^{-4} \partial_\alpha^2, \\
L_{22} &:= 1 + \frac{c\tau_1 M^2}{4\pi^2 S} \left(\frac{A\bar{\gamma}}{\tau_1} - \frac{cM}{\pi \tau_1} \right) H \partial_\alpha^{-4} \partial_\alpha.
\end{aligned}$$

3.2.4. *Eigenvalue calculation.* The next step in applying Theorem 8 to $(\theta - \Theta, \gamma_1 - \Gamma)$ is to find c that yield zero eigenvalues of L_c . To do so, we note the periodicity of $(\vec{\theta}, \vec{\gamma})$, and examine the Fourier coefficients of L_c . Let μ be a general 2π -periodic map with convergent Fourier series. Noting our definition of $\widehat{\partial_\alpha^{-4} \mu}(k)$ in (21), along with the elementary results

$$\begin{aligned}
\widehat{\partial_\alpha \mu}(k) &= ik \widehat{\mu}(k), \\
\widehat{\partial_\alpha^2 \mu}(k) &= -k^2 \widehat{\mu}(k), \\
\widehat{H \mu}(k) &= -i \operatorname{sgn}(k) \widehat{\mu}(k), \\
\widehat{P \mu}(k) &= (1 - \delta_0(k)) \widehat{\mu}(k),
\end{aligned}$$

we compute, for $k \neq 0$,

$$\begin{aligned}
\widehat{L_{11}}(k) &= 1 - \frac{\tau_1 \bar{\gamma} M}{4\pi S} \left(\frac{\bar{\gamma}}{\tau_1} - \frac{cAM}{\pi \tau_1} \right) \frac{1}{|k|^3} + \frac{AM^4}{8\pi^4 S} \frac{1}{k^4} + \frac{\tau_1 M^2}{4\pi^2} \frac{1}{k^2}, \\
\widehat{L_{12}}(k) &= i \frac{\tau_1 M^2}{4\pi^2 S} \left(\frac{\pi A \bar{\gamma}}{\tau_1 M} - \frac{c}{\tau_1} \right) \frac{1}{k^3}, \\
\widehat{L_{21}}(k) &= i \frac{c\tau_1 \bar{\gamma} M^2}{4\pi^2 S} \left(\frac{\bar{\gamma}}{\tau_1} - \frac{cAM}{\pi \tau_1} \right) \frac{1}{k^3} - i \frac{cAM^5}{8\pi^5 S} \frac{\operatorname{sgn}(k)}{k^4} - i \frac{c\tau_1 M^3}{4\pi^3} \frac{\operatorname{sgn}(k)}{k^2}, \\
\widehat{L_{22}}(k) &= 1 + \frac{c\tau_1 M^2}{4\pi^2 S} \left(\frac{A\bar{\gamma}}{\tau_1} - \frac{cM}{\pi \tau_1} \right) \frac{1}{|k|^3};
\end{aligned}$$

thus,

$$L_c \begin{bmatrix} \vec{\theta} \\ \vec{\gamma} \end{bmatrix} (k) = \widehat{L}_c(k) \begin{bmatrix} \vec{\theta} \\ \vec{\gamma} \end{bmatrix} = \begin{bmatrix} \widehat{L_{11}}(k) & \widehat{L_{12}}(k) \\ \widehat{L_{21}}(k) & \widehat{L_{22}}(k) \end{bmatrix} \begin{bmatrix} \vec{\theta} \\ \vec{\gamma} \end{bmatrix}.$$

For $k = 0$, $\widehat{P \mu}(k) = 0$, so $\widehat{L}_c(0) = I$. Clearly, when $k = 0$, 1 is an eigenvalue with multiplicity 2. For $k \neq 0$, we compute the eigenvalues via Mathematica [31]. In this case, 1 is also an eigenvalue, as is

$$\lambda_k(c) := 1 + \frac{M^2 \tau_1}{4\pi^2} |k|^{-2} + \frac{-c^2 M^3 + 2Ac\bar{\gamma} M^2 \pi - \bar{\gamma}^2 M \pi^2}{4\pi^3 S} |k|^{-3} + \frac{AM^4}{8\pi^4 S} |k|^{-4}.$$

Note that $\lambda_k(c)$ is even with respect to k . Also, by basic Fourier series results, $\{1\} \cup \{\lambda_k(c)\}_k$ constitutes the point spectrum of L_c . The eigenvector corresponding to $\lambda_k(c)$ is

$$(32) \quad v_k(c) := \begin{bmatrix} \frac{\operatorname{sgn}(k) i \pi}{cM} \\ 1 \end{bmatrix},$$

and thus

$$\begin{bmatrix} \frac{i\pi}{cM} \\ 1 \end{bmatrix} \exp(ik\alpha) \quad \text{and} \quad \begin{bmatrix} -\frac{i\pi}{cM} \\ 1 \end{bmatrix} \exp(-ik\alpha).$$

are each eigenfunctions of L_c . However, we can take real and imaginary parts of each, and obtain eigenfunctions

$$\begin{bmatrix} -\frac{\pi}{cM} \sin(k\alpha) \\ \cos(k\alpha) \end{bmatrix} \quad \text{and} \quad \begin{bmatrix} \frac{\pi}{cM} \cos(k\alpha) \\ \sin(k\alpha) \end{bmatrix}.$$

Only the first is in $H_{\text{per,odd}}^2 \times H_{\text{per,0,even}}^1$, thus, given our chosen function space, we have that the dimension of the eigenspace of $\lambda_k(c)$ is one. We can then drop the absolute values, and state, for $k > 0$,

$$(33) \quad \lambda_k(c) = 1 + \frac{M^2\tau_1}{4\pi^2} k^{-2} + \frac{-c^2 M^3 + 2Ac\bar{\gamma}M^2\pi - \bar{\gamma}^2 M\pi^2}{4\pi^3 S} k^{-3} + \frac{AM^4}{8\pi^4 S} k^{-4}.$$

We summarize the spectral results thus far, along with with a few immediate consequences, below:

Proposition 12. *Let L_c be the linearization of $(\theta, \gamma_1; c) \mapsto (\theta - \Theta(\theta, \gamma_1; c), \gamma_1 - \Gamma(\theta, \gamma_1; c))$ at $(0, 0; c)$. The spectrum of L_c is the set of eigenvalues $\{1\} \cup \{\lambda_k(c) : k \in \mathbb{N}\}$, where $\lambda_k(c)$ is as defined in (33). Each eigenvalue λ of L_c has algebraic multiplicity equal to its geometric multiplicity, which we denote*

$$N_\lambda(c) := |\{k \in \mathbb{N} : \lambda_k(c) = \lambda\}|,$$

and the corresponding eigenspace is

$$E_\lambda(c) := \text{span} \left\{ \begin{bmatrix} -\frac{\pi}{cM} \sin(k\alpha) \\ \cos(k\alpha) \end{bmatrix} : k \in \mathbb{N} \text{ such that } \lambda_k(c) = \lambda \right\}.$$

Also, for fixed k , if the inequality

$$(34) \quad AM^4 + (-2\bar{\gamma}^2 M\pi^3 + 2A^2\bar{\gamma}^2 M\pi^3)k + 2M^2\pi^2 S\tau_1 k^2 + 8\pi^4 S k^4 \geq 0$$

holds, then the $c \in \mathbb{R}$ for which $\lambda_k(c) = 0$ is

$$(35) \quad c_\pm(k) := \frac{A\bar{\gamma}\pi}{M} \pm \sqrt{\frac{AM^4 + (-2\bar{\gamma}^2 M\pi^3 + 2A^2\bar{\gamma}^2 M\pi^3)k + 2M^2\pi^2 S\tau_1 k^2 + 8\pi^4 S k^4}{2kM^3\pi}},$$

and this zero eigenvalue has multiplicity $N_0(c_\pm(k)) \leq 2$. Specifically, if we define the polynomial (in l)

$$p(l; k) := -AM^4 + 2kl\pi^2 S (4(k^2 + kl + l^2)\pi^2 + M^2\tau_1),$$

$p(\cdot; k)$ has a single real root (denoted $l(k)$), and we have $N_0(c_\pm(k)) = 2$ if and only if $l(k)$ is a positive integer not equal to k .

Proof. The point spectrum of L_c , along with each $E_\lambda(c)$, was explicitly calculated above. The fact that the the geometric and algebraic multiplicities are equal follows from the even/odd considerations of the eigenfunctions.

The result (35) follows from an easy computation, as $\lambda_k(c)$ is quadratic in c . Next, we wish to make statements about the multiplicity of the zero eigenvalue $\lambda_k(c_\pm(k))$. Using (33) and (35), we compute

$$(36) \quad \lambda_l(c_\pm(k)) = -\frac{(k-l)(-AM^4 + 2kl\pi^2 S (4(k^2 + kl + l^2)\pi^2 + M^2\tau_1))}{8kl^4\pi^4 S}.$$

Obviously, $\lambda_l(c_\pm(k)) = 0$ when $l = k$. The other factor in the numerator of $\lambda_l(c_\pm(k))$ is precisely the polynomial p defined above, which is cubic in l . Using Mathematica, we compute its three roots, and label them $l_1(k)$, $l_2(k)$, $l_3(k)$:

$$\begin{aligned} l_1(k) &:= \frac{-B + 4k^{8/3}\pi^{4/3}S^{5/3}\left(C + 3\sqrt{3}\sqrt{D}\right)^{1/3} + \left(2k^2S^2\left(C + 3\sqrt{3}\sqrt{D}\right)\right)^{2/3}}{12\pi^{4/3}(kS)^{5/3}\left(C + 3\sqrt{3}\sqrt{D}\right)^{1/3}}, \\ l_2(k) &:= \frac{zB - 8k^{8/3}\pi^{4/3}S^{5/3}\left(C + 3\sqrt{3}\sqrt{D}\right)^{1/3} - \bar{z}\left(2k^2S^2\left(C + 3\sqrt{3}\sqrt{D}\right)\right)^{2/3}}{24\pi(kS)^{5/3}\left(C + 3\sqrt{3}\sqrt{D}\right)^{1/3}}, \\ l_3(k) &:= \overline{l_2(k)}, \end{aligned}$$

where

$$\begin{aligned} z &:= 1 + i\sqrt{3}, \\ B &:= 2 \cdot 2^{1/3}k^2S^2\left(8\pi^{8/3}k^2 + 3M^2\pi^{2/3}\tau_1\right), \\ C &:= 27AM^4 + 56k^4\pi^4S + 18k^2M^2\pi^2S\tau_1, \\ D &:= 27A^2M^2 + 4k^2\pi^2S^2\left(3k^2\pi^2 + M^2\tau_1\right)\left(4k^2\pi^2 + M^2\tau_1\right)^2 \\ &\quad + 4Ak^2M^4\pi^2S\left(28k^2\pi^2 + 9M^2\tau_1\right). \end{aligned}$$

We see $D > 0$ given the nature of the constants in our problem; also, we have $B, C \in \mathbb{R}$, so $l_1(k)$ is real. For $l_2(k)$ to be real, we would need

$$\operatorname{Im}\left[zB - \bar{z}\left(2k^2S^2\left(C + 3\sqrt{3}\sqrt{D}\right)\right)^{2/3}\right] = 0.$$

But,

$$\begin{aligned} &\operatorname{Im}\left[zB - \bar{z}\left(2k^2S^2\left(C + 3\sqrt{3}\sqrt{D}\right)\right)^{2/3}\right] \\ &= \sqrt{3}\left[B + \left(2k^2S^2\left(C + 3\sqrt{3}\sqrt{D}\right)\right)^{2/3}\right] \end{aligned}$$

Thus, for $l_2(k)$ to be real, we would need

$$B = -\left(2k^2S^2\left(C + 3\sqrt{3}\sqrt{D}\right)\right)^{2/3},$$

Since $S > 0, k > 0$, we see that B is always positive, yet the right-hand-side is always negative (recall that $D > 0$). Thus, $l_2(k)$ (and, subsequently, $l_3(k)$ as well) necessarily has nonzero imaginary part, and hence cannot be an integer. Therefore, when counting the multiplicity of zero eigenvalues of L_c , we only need to consider the real root $l_1(k)$, which we label as $l(k)$. Given k such that (34) holds, we have that $N_0(c_\pm(k)) \leq 2$, since p has one real root $l(k)$.

If $l(k) \neq k$ is a positive integer, then we clearly have $N_0(c_\pm(k)) = 2$ (since in this case both k and $l(k)$ – and only these two positive integers – correspond to the same zero eigenvalue). Conversely, if $N_0(c_\pm(k)) = 2$, then the right-hand-side of (36) must have a positive integer root $l \neq k$, and we established that such l must be the real root $l(k)$ of the polynomial p . ■

With this spectral information at hand, we are now ready to make some statements about the crossing number of L_c .

3.2.5. Necessary and sufficient conditions for odd crossing number.

Proposition 13. *Fix constants $A \in [-1, 1]$, $\bar{\gamma} \in \mathbb{R}$ and $S, \tau_1, M > 0$. Define the mapping $(\theta - \Theta, \gamma - \Gamma)$ as before, and let L_c be its linearization at $(0, 0; c)$. Given fixed k , define $c_{\pm}(k)$ and $l(k)$ as in Proposition 12. Further, put*

$$(37) \quad K := \{k \in \mathbb{N} \quad : \quad AM^4 + (-2\bar{\gamma}^2 M\pi^3 + 2A^2\bar{\gamma}^2 M\pi^3)k + 2M^2\pi^2 S\tau_1 k^2 + 8\pi^4 S k^4 > 0 \\ \text{and } l(k) \notin \mathbb{N} \setminus \{k\}\}.$$

Then, L_c has an odd crossing number (specifically, the crossing number is one) at $c = c_{\pm}(k)$ (which is real) if and only if $k \in K$. Furthermore, $|K| = \infty$.

Proof. First, assume $k \in K$. The first condition in the definition of K ensures (34) holds in Proposition 12, so we have that $c = c_{\pm}(k)$ is real, and yields a zero eigenvalue of L_c , so $N_0(c_{\pm}(k)) \geq 1$. The second condition ensures that $N_0(c_{\pm}(k)) < 2$ by the last conclusion of Proposition 12. Thus, $N_0(c_{\pm}(k)) = 1$.

For a direct calculation of the crossing number, we examine a perturbation of this zero eigenvalue, computed via Mathematica:

$$(38) \quad \lambda_k(c_{\pm}(k) + \varepsilon) \\ = \mp \frac{M^3}{2k^3\pi^3 S} \sqrt{\frac{AM^4 + (-2\bar{\gamma}^2 M\pi^3 + 2A^2\bar{\gamma}^2 M\pi^3)k + 2M^2\pi^2 S\tau_1 k^2 + 8\pi^4 S k^4}{2kM^3\pi}} \varepsilon \\ - \frac{M^3}{4k^3\pi^3 S} \varepsilon^2.$$

Note that this expression is exact, since from (33) we have that $\lambda_k(c)$ is quadratic in c . Also, in the leading-order term of (38), the expression under the radical is identical to that which is under the radical of (35); yet, we have a strict inequality in the first condition in the definition of K . Thus, since this leading-order coefficient is positive, we see that $\lambda_k(c_{\pm}(k) + \varepsilon)$ changes sign as ε passes over zero. Since we have a multiplicity of one, we see that there is an odd crossing number at $c = c_{\pm}(k)$ from a direct application of Definition 6 (and this crossing number is in fact one, as exactly one eigenvalue, counted with multiplicity, is changing sign as ε passes over zero).

Now, assume an odd crossing number at a real $c = c_{\pm}(k)$ for some $k \in \mathbb{N}$. By definition of $c_{\pm}(k)$, we have $N_0(c_{\pm}(k)) \geq 1$, and by Proposition 12, we have $N_0(c_{\pm}(k)) \leq 2$. Thus, either $N_0(c_{\pm}(k)) = 1$ or $N_0(c_{\pm}(k)) = 2$. We show that the former implies $k \in K$, and that the latter leads to a contradiction. In the case $N_0(c_{\pm}(k)) = 1$, we necessarily have $l(k) \notin \mathbb{N} \setminus \{k\}$; otherwise, the multiplicity would be 2. Moreover, $c_{\pm}(k)$ must be real, and since the crossing number is odd, $\lambda_k(c_{\pm}(k) + \varepsilon)$ (which is the only eigenvalue perturbing from the zero eigenvalue, assumed in this case to be of multiplicity 1) must change sign as ε passes over 0. Thus, by the same calculation (38), we need the leading-order term to be nonzero, which forces the strict inequality in the first condition in the definition of K . Thus, we have $k \in K$.

If $N_0(c_{\pm}(k)) = 2$, then clearly $l(k) \neq k$ is a positive integer. A Mathematica calculation shows

$$\begin{aligned}
 (39) \quad & \lambda_{l(k)}(c_{\pm}(k) + \varepsilon) \\
 = & -\frac{(k - l(k))(-AM^4 + 2kl(k)\pi^2 S(4(k^2 + kl(k) + [l(k)]^2)\pi^2 + M^2\tau_1))}{8k[l(k)]^4\pi^4 S} \\
 & \mp \frac{M^3}{2[l(k)]^3\pi^3 S} \sqrt{\frac{AM^4 + (-2\bar{\gamma}^2 M\pi^3 + 2A^2\bar{\gamma}^2 M\pi^3)k + 2M^2\pi^2 S\tau_1 k^2 + 8\pi^4 S k^4}{2kM^3\pi}} \varepsilon \\
 & - \frac{M^3}{4[l(k)]^3\pi^3 S} \varepsilon^2.
 \end{aligned}$$

As expected, the zeroth-order (in ε) term of (39) is precisely $\lambda_{l(k)}(c_{\pm}(k))$ (see (36)), which vanishes by definition of $l(k)$. Then, we can see that the first-order term of (39) is real and nonzero if and only if the first-order term of (38) is real and nonzero. Thus, as ε passes over zero, either (i) both $\lambda_k(c_{\pm}(k) + \varepsilon)$ and $\lambda_{l(k)}(c_{\pm}(k) + \varepsilon)$ change signs, or (ii) neither of them change signs. In either case, we cannot have an odd crossing number, which contradicts our assumption.

Finally, we need to show that $|K| = \infty$. First, we see that $8\pi^4 S$ is positive, so for sufficiently large k , the first condition in the definition of K is satisfied. For the second condition, we need to check the behavior of $l(k)$. Perform the substitution $k = 1/\delta$ ($\delta > 0$), and examine the Taylor series expansion of $l(1/\delta)$ about $\delta = 0$ (computed via Mathematica):

$$l\left(\frac{1}{\delta}\right) = \frac{AM^4}{8\pi^4 S} \delta^3 + O(\delta^5).$$

We see that

$$\lim_{\delta \rightarrow 0} l\left(\frac{1}{\delta}\right) = 0,$$

so

$$\lim_{k \rightarrow \infty} l(k) = 0$$

as well. Thus, for sufficiently large k , the second condition in the definition of K holds. Since both the first and second conditions hold for sufficiently large k , we have that $|K| = \infty$. ■

Remark 14. *There are other, “indirect” methods for providing sufficient conditions for an odd crossing number. One result, which appears in [15], states that if 0 is a geometrically simple eigenvalue of $D_x F(0, c_0)$, and*

$$(40) \quad \left(Q \left[\frac{d}{dc} D_x F(0, c) \right]_{c=c_0} \right) v \neq 0,$$

where v is an arbitrary element of the null space of $D_x F(0, c_0)$, and Q is the projection onto the cokernel of $D_x F(0, c_0)$ (note the dimensions in this case are such that the left-hand side is a scalar quantity), then $D_x F(0, c)$ has an odd crossing number at $c = c_0$. For our problem, we note that for matrices A , $\text{coker}(A) =$

$\ker(A^*)$, and thus we examine

$$(41) \quad w_k(c_0) \cdot \left(\left[\frac{d}{dc} \widehat{L}_c(k) \right]_{c=c_0} v_k(c_0) \right)$$

where $v_k(c_0)$ is as defined in (32), $w_k(c_0)$ is the eigenvector corresponding to the zero eigenvalue of $\left[\widehat{L}_{c_0}(k) \right]^*$, and the dot indicates the usual Euclidean dot product.

We arrive at precisely the same condition for (41) to be nonzero as the strict inequality in the the definition of K (37). This, coupled with the assumption that the null space is one-dimensional, allows us to conclude that if $k \in K$, then the crossing number is odd. Unfortunately, (40) is stated as only a sufficient condition for odd crossing number, and so we could not conclude the “only if” direction of Proposition 13 by using this method alone. Because of this, and because the nature of the problem fortunately allowed for the method to be manageable and conclusive, we favored a “direct” verification of an odd crossing number (namely calculations (38) and (39)).

3.2.6. Global bifurcation conclusion. We can now apply Theorem 8, and cast the conclusions of this abstract theorem in the language of our problem.

Theorem 15. Define $U_{0,0} := \cup_{b,h>0} U_{b,h}$, where $U_{b,h}$ is as defined in (30). Let $S \subseteq U_{0,0}$ be the closure (in $H^2_{per,odd} \times H^1_{per,0,even} \times \mathbb{R}$) of the set of nontrivial (i.e. θ, γ_1 are not both zero) solutions of the traveling wave problem $(\theta - \Theta(\theta, \gamma_1; c), \gamma_1 - \Gamma(\theta, \gamma_1; c)) = 0$. Furthermore, let $c_{\pm}(k)$ and K be as in Propositions 12 and 13. For fixed $k \in K$, define $C_{\pm}(k)$ to be the connected component of S that contains $(0, 0; c_{\pm}(k))$. Then, one of the following alternatives is valid:

- (I): $C_{\pm}(k)$ is unbounded; or
- (II): $C_{\pm}(k) = C_+(j)$ or $C_{\pm}(k) = C_-(j)$ for some $j \in K$ with $j \neq k$; or
- (III): $C_{\pm}(k)$ contains a point on the boundary of $U_{0,0}$.

Proof. Assume $k \in K$. Given $b, h > 0$, we have by Proposition 11 that (Θ, Γ) is compact on $U_{b,h}$, and by Proposition 13, there is an odd crossing number of the linearization at $c = c_{\pm}(k)$. Since the conditions for Theorem 8 are met, we can conclude that one of outcomes (i), (ii), (iii) in the conclusion of this theorem occur (using $U = U_{b,h}$). The outcomes (i) (ii) correspond exactly with outcomes (I), (II) above. Taking a union over all $b, h > 0$, outcome (iii) yields outcome (III) above via a simple topological argument. ■

3.3. Proof of main theorem. We are now ready to prove Theorem 4. With the bifurcation results of Theorem 15 at hand, this proof will largely be comprised of matching the outcomes (I) – (III) above with the outcomes (a) – (e) in Theorem 4. Many of these conclusions can be reached through arguments identical to (or closely analogous to) those in [9].

Proof. First, note that Proposition 13 gives us that $|K| = \infty$; hence, by Theorem 15, we have a countable number of connected sets of the form $C_{\pm}(k)$ ($k \in K$) that satisfy one of outcomes (I) – (III).

We can immediately see that Outcome (II) means (e).

Next, consider Outcome (III). Recall the definition of $U_{0,0}$ in Theorem 15, and note that we can write

$$U_{0,0} = \left\{ (\theta, \gamma_1; c) \in X : \overline{\cos \theta} > 0, \tilde{Z}[\theta] \in C_0^2 \text{ and } \tilde{Z}[\Theta(\theta, \gamma_1; c)] \in C_0^5 \right\},$$

where

$$X = H_{\text{per,odd}}^2 \times H_{\text{per,0,even}}^1 \times \mathbb{R}.$$

Outcome (III) means either $\overline{\cos \theta} = 0$ or $\tilde{Z}[\theta] = \tilde{Z}[\Theta(\theta, \gamma_1; c)] \notin C_0^5$. As in [9], $\overline{\cos \theta} = 0$ implies (a). If $\tilde{Z}[\theta] \notin C_0^5$, we have that the interface self-intersects by the same argument as in [9] (the $s = 5$ regularity does not affect this argument). This is outcome (d).

Outcome (I) (i.e. unboundedness of the solution set) can lead to more outcomes in this main theorem. If $C_{\pm}(k)$ is unbounded, then it contains a sequence of solutions $(\theta_n, \gamma_{1,n}; c_n)$ in U such that

$$(42) \quad \lim_{n \rightarrow \infty} \left(|c_n| + \|\theta_n\|_{H_{\text{per}}^2} + \|\gamma_{1,n}\|_{H_{\text{per}}^1} \right) = \infty.$$

We first note that, as in [9], if (a) does not hold, then σ_n is bounded above independently of n . For the remainder of this proof, assume (a) does not hold, and hence σ_n is bounded above independently of n . At least one of the three terms of (42) must diverge; we subsequently examine each case.

If $|c_n| \rightarrow \infty$, yet $\|\theta_n\|_{H_{\text{per}}^2} + \|\gamma_{1,n}\|_{H_{\text{per}}^1}$ is bounded, then either $\bar{\gamma} \neq 0$ or $A \neq 0$ are violated as in [9] (yet $|c_n| \rightarrow \infty$ is outcome (f), which may possible, independent of the other outcomes, when $\bar{\gamma} = 0$ and $A = 0$). To see this, first recall that (17) implies

$$\|c_n \sin(\theta_n)\|_{H^2} = \|\text{Re}(W_n^* N_n)\|_{H^2}.$$

Lemma 5 of [9] shows us that the right-hand side is bounded, so we have that $c_n \sin(\theta_n)$ is bounded in H^2 . Since by assumption $|c_n| \rightarrow \infty$, this forces $\|\sin(\theta_n)\|_{H_{\text{per}}^2}$ to approach 0; then, by Sobolev embedding, we have $\sin(\theta_n) \rightarrow 0$ uniformly. Thus, θ_n must converge to a multiple of π ; but, by continuity and the fact that θ is an odd function, we have $\theta_n \rightarrow 0$ uniformly, and clearly $|\cos(\theta_n)| \rightarrow 1$ (uniformly) as well.

Now, recall (11):

$$\begin{aligned} 0 &= -\frac{S}{\tau_1 \sigma^2} \left(\partial_{\alpha}^A \theta + \frac{3\theta_{\alpha}^2 \theta_{\alpha\alpha}}{2} - \tau_1 \sigma^2 \theta_{\alpha\alpha} \right) - \frac{2\tilde{A}\sigma}{\tau_1} (\cos \theta)_{\alpha} \\ &\quad + \frac{1}{\tau_1} ((c \cos \theta - \text{Re}(W^* T)) \gamma)_{\alpha} \\ &\quad - \frac{A}{\tau_1} \left(\frac{\partial_{\alpha}(\gamma^2)}{4\sigma} + 2\sigma \sin \theta + \sigma \partial_{\alpha} \left\{ (c \cos \theta - \text{Re}(W^* T))^2 \right\} \right), \end{aligned}$$

or

$$\begin{aligned} 0 &= S \left(-\frac{\partial_{\alpha}^A \theta}{\sigma^2} - \frac{3\theta_{\alpha}^2 \theta_{\alpha\alpha}}{2\sigma^2} + \tau_1 \theta_{\alpha\alpha} \right) - 2\tilde{A}\sigma (\cos \theta)_{\alpha} \\ &\quad + ((c \cos \theta - \text{Re}(W^* T)) \gamma)_{\alpha} \\ &\quad - 2A \left(\frac{\partial_{\alpha}(\gamma^2)}{\sigma} + \sigma^2 \sin \theta + \frac{1}{2} \sigma \partial_{\alpha} \left\{ (c \cos \theta - \text{Re}(W^* T))^2 \right\} \right). \end{aligned}$$

We integrate twice with respect to α , and substitute our sequences of solutions:

$$\begin{aligned} 0 &= S \left(-\frac{\partial_\alpha^2 \theta_n}{\sigma_n^2} - \int \frac{(\partial_\alpha \theta_n)^3}{2\sigma^2} d\alpha + \tau_1 \theta_n \right) - 2\tilde{A}\sigma_n \int \cos \theta_n d\alpha \\ &\quad + \int (c_n \cos \theta_n - \operatorname{Re}(W^*T)) \gamma_n d\alpha \\ &\quad - 2A \int \left\{ \left[\frac{1}{8} \frac{\gamma_n^2}{\sigma_n} + \sigma_n^2 \int \sin \theta_n d\alpha + \frac{\sigma_n}{2} (c_n \cos \theta_n - \operatorname{Re}(W_n^*T_n))^2 \right] \right\} d\alpha. \end{aligned}$$

Given that $\|\theta_n\|_{H_{\text{per}}^2}$ is bounded, we have that

$$S \left(-\frac{\partial_\alpha^2 \theta_n}{\sigma_n^2} - \int \frac{(\partial_\alpha \theta_n)^3}{2\sigma^2} d\alpha + \tau_1 \theta_n \right)$$

is bounded in L_{per}^2 , as is the ‘‘mass’’ term

$$2\tilde{A}\sigma_n \int \cos \theta_n d\alpha.$$

Thus,

$$(43) \quad \int (c_n \cos \theta_n - \operatorname{Re}(W^*T)) \gamma_n d\alpha - 2A \int \left\{ \left[\frac{1}{8} \frac{\gamma_n^2}{\sigma_n} + \sigma_n^2 \int \sin \theta_n d\alpha + \frac{\sigma_n}{2} (c_n \cos \theta_n - \operatorname{Re}(W_n^*T_n))^2 \right] \right\} d\alpha$$

must be bounded in L_{per}^2 .

Now, assume that $A = 0$. With this assumption, we are left with the conclusion that

$$\int (c_n \cos \theta_n - \operatorname{Re}(W^*T)) \gamma_n d\alpha$$

is bounded in L_{per}^2 . Again, Lemma 5 of [9] shows $\operatorname{Re}(W^*T)$ is bounded in H_{per}^1 , so since γ_n is also assumed to be bounded in H_{per}^1 , we have that

$$\int \operatorname{Re}(W^*T) \gamma_n d\alpha$$

is bounded in H_{per}^2 , and hence is also bounded in L_{per}^2 . Thus,

$$\int c_n \cos(\theta_n) \gamma_n d\alpha$$

is subsequently bounded in L_{per}^2 as well. Since $c_n \rightarrow \infty$, this forces

$$\int \gamma_n d\alpha \rightarrow 0 \quad (\text{in } L_{\text{per}}^2).$$

However, we can write $\gamma_n = \gamma_{1,n} + \bar{\gamma}$, where $\gamma_{1,n}$ has mean zero. Since

$$\int \gamma_{1,n} d\alpha \rightarrow 0 \quad (\text{in } L^2_{\text{per}}),$$

we need

$$\int \bar{\gamma} d\alpha = \bar{\gamma} \alpha \rightarrow 0 \quad (\text{in } L^2_{\text{per}}).$$

This forces $\bar{\gamma} = 0$.

Now, suppose $A \neq 0$. Divide (43) by c_n^2 :

$$(44) \quad \int \left(\frac{1}{c_n} \cos \theta_n - \frac{1}{c_n^2} \operatorname{Re}(W^* T) \right) \gamma_n d\alpha \\ - 2A \int \left\{ \left[\frac{1}{8} \frac{\gamma_n^2}{c_n^2 \sigma_n} + \frac{\sigma_n^2}{c_n^2} \int \sin \theta_n d\alpha + \frac{\sigma_n}{2c_n^2} (c_n \cos \theta_n - \operatorname{Re}(W_n^* T_n))^2 \right] \right\} d\alpha.$$

Since (43) is bounded in L^2_{per} , we have that (44) must approach 0. Examining each term of (44), we see that all but possibly

$$\int \frac{\sigma_n}{2c_n^2} (c_n \cos \theta_n - \operatorname{Re}(W_n^* T_n))^2 d\alpha$$

clearly approach 0. After expanding the integrand, we see that all terms would in fact approach zero on their own merit except for the leading-order (in c_n) term

$$\int \frac{\sigma_n}{2c_n^2} c_n^2 \cos^2 \theta_n d\alpha = \frac{1}{2} \int \sigma_n \cos^2 \theta_n d\alpha.$$

Since all other terms of (44) approaches zero, this forces

$$\frac{1}{2} \int \sigma_n \cos^2 \theta_n d\alpha \rightarrow 0.$$

Thus,

$$\sigma_n \cos^2 \theta_n \rightarrow 0,$$

which is a contradiction, since $|\cos \theta_n| \rightarrow 1$ from earlier.

In whole, we have a contradiction between the statements (i) $|c_n| \rightarrow \infty$ but $\|\theta_n\|_{H^2_{\text{per}}} + \|\gamma_{1,n}\|_{H^1_{\text{per}}}$ is bounded, and (ii) either $\bar{\gamma} \neq 0$ or $A \neq 0$. Thus, if we assume either $\bar{\gamma} \neq 0$ or $A \neq 0$ and $|c_n| \rightarrow \infty$, we must necessarily have $\|\theta_n\|_{H^2_{\text{per}}} + \|\gamma_{1,n}\|_{H^1_{\text{per}}}$ additionally unbounded; hence, in this case, outcome (f) implies other outcomes as in the [9]. But, if both $A = 0$ and $\bar{\gamma} = 0$, we do not exclude the possibility $|c_n| \rightarrow \infty$ but $\|\theta_n\|_{H^2_{\text{per}}} + \|\gamma_{1,n}\|_{H^1_{\text{per}}}$ is bounded, so we list (f) as another possible outcome.

With the case $|c_n| \rightarrow \infty$ handled, we now turn our attention to the case in which $\|\theta_n\|_{H^2_{\text{per}}}$ (the second term of (42)) diverges. This means that one of θ_n , $\partial_\alpha \theta_n$, or $\partial_\alpha^2 \theta_n$ diverge. Recall that $\kappa(\alpha) = \partial_\alpha \theta(\alpha) / \sigma$, so $\partial_\alpha \kappa(\alpha) = \partial_\alpha^2 \theta(\alpha) / \sigma$. Since

$$2\pi \overline{\cos \theta} = \int_0^{2\pi} \cos(\theta(\alpha')) d\alpha' = \frac{M}{\sigma},$$

we cannot have $\sigma_n \rightarrow 0$. Since σ_n is bounded above as well, then if $\partial_\alpha^2 \theta_n$ diverges, then so does the derivative of curvature. This is outcome (b).

Finally, it is shown in [9] that $\|\gamma_{1,n}\|_{H_{\text{per}}^1} \rightarrow \infty$ implies either outcome (a) or outcome (c).

Note that if curvature or the jump of the tangential component of fluid velocity themselves are arbitrarily large, then (respectively) (b) or (c) occur as well, so we omit these as separate outcomes. ■

In the next section, we proceed to numerically compute some of these diverse solution curves.

4. NUMERICAL METHODS AND RESULTS

4.1. Methods. For our numerical computations, we employ methods very similar to those in [2]. Our computations use the version of our equations given by (12) and (17). We specify the horizontal domain width $M = 2\pi$ ($\alpha \in [-\pi, \pi]$), and project each of θ, γ onto a finite-dimensional Fourier space:

$$\theta(\alpha) = \sum_{k=-N}^{k=N} a_k \exp(ik\alpha), \quad \gamma(\alpha) = \sum_{k=-N}^{k=N} b_k \exp(ik\alpha).$$

As in the formulation of our problem, we work with odd, real θ and even, real γ . This forces $a_{-k} = -a_k$ (so $a_0 = 0$) and $b_{-k} = b_k$ (and clearly $b_0 = \bar{\gamma}$). Thus, with $\bar{\gamma}$ specified *a priori*, we can see that a traveling wave solution $(\theta, \gamma; c)$ is determined by the $2N$ coefficients $a_1, \dots, a_N, b_1, \dots, b_N$, along with the wave speed c . To solve for these $2N + 1$ values, we project both sides of equations (12), (17) onto each basis element $\exp(ik\alpha)$, $1 \leq k \leq N$. This yields a system of $2N$ algebraic equations; to complete the system, we include another equation that allows us to specify the amplitude of the solution.

The most difficult, non-obvious portion of the computation of these algebraic equations is, perhaps, the computation of the Birkhoff-Rott integral W^* in Fourier space. However, as in [9] (and what was used in our “identity plus compact” formulation (27), (28)), we can write W^* as the sum

$$W^* = \frac{1}{2}H\left(\frac{\gamma}{z_\alpha}\right) + \mathcal{K}[z]\gamma,$$

where, as before, H is the Hilbert transform, and the remainder $\mathcal{K}[z]\gamma$ can be explicitly written as

$$\mathcal{K}[z]\gamma(\alpha) = \frac{1}{4\pi i} \text{PV} \int_0^{2\pi} \gamma(\alpha') \left[\cot\left(\frac{1}{2}(z(\alpha) - z(\alpha'))\right) - \frac{1}{\partial_{\alpha'} z(\alpha')} \cot\left(\frac{1}{2}(\alpha - \alpha')\right) \right] d\alpha'.$$

The Hilbert transform H is easily computed in Fourier space, as

$$\widehat{H\mu}(k) = -i \operatorname{sgn}(k) \widehat{\mu}(k).$$

The remainder $\mathcal{K}[z]\gamma$ is computed with the trapezoid rule, in an “alternating” sense (i.e. to evaluate this integral at an “even” grid point, we sum the “odd” nodes, and vice-versa).

We proceed to numerically solve these $2N + 1$ algebraic equations with Broyden’s method (a quasi-Newton method which approximates the Jacobian of the system with a rank-one update to the Jacobian at the previous iteration; see [12]). A

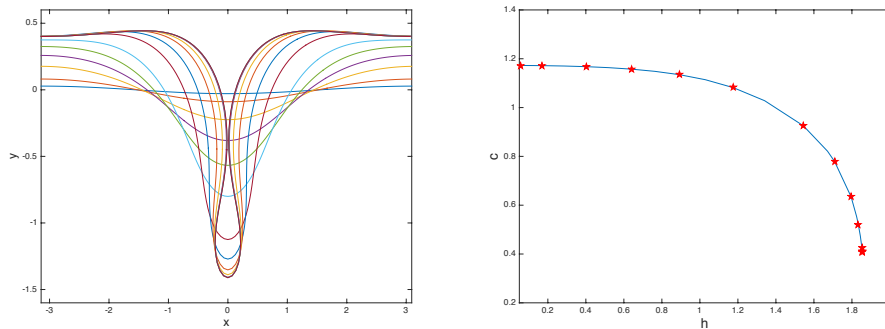


FIGURE 1. An example computation of an entire branch of traveling waves, with $S = 0.25$, $\tau = 2$, $A = 1$ and $\tilde{A} = 0.2$. A sampling of wave profiles at different locations on the branch are depicted in the left panel. These profiles are marked with stars on the speed amplitude curve in the right panel. The branch terminates with a self-intersecting profile.

small-amplitude solution to the linearized equations (31) (with linear wave speed c_{\pm} given by (35)) is used as the initial guess for Broyden’s method, where amplitude (displacement) is specified as the y -coordinate of the free-surface at the central node $x = 0$. After iterating to a solution within a desired tolerance, we record the solution.

Then, as is typically done in these types of continuation methods, we look for more solutions along the same branch by perturbing the previously computed solution by a small amount in some direction, then using this perturbation as an initial guess for the next application of Broyden’s method. The perturbation direction is called the continuation parameter. We begin using total displacement as the continuation parameter. If a given “step size” of displacement does not yield convergence, then we choose a smaller (i.e. halve the previous step size) perturbation from the last known solution as an initial guess. However, if the step size drops below a given threshold, we switch to using a Fourier mode as our continuation parameter. If the step size for this continuation process becomes to small, we subsequently continue in higher Fourier modes.

We follow a branch of solutions until the solution self-intersects (i.e. outcome (d) of Theorem 4), returns to the trivial solution (i.e. outcome (e)), or becomes to large to resolve (evidence of outcome (a)). After any such termination criterion is achieved, we cease the continuation process, and record all solutions along the branch. An example of a computed branch of waves which terminates in self-intersection is in Figure 1.

4.2. Results. In this section we present computations of global branches of traveling hydroelastic waves. Global branches are computed which terminate in a self-intersecting profile, as well as branches whose most extreme representative is a standing wave, $c = 0$. We pay particular focus to the role of \tilde{A} , a proxy for the mass of the ice sheet. This parameter was chosen as it appears only in the nonlinearity; the linear speeds and infinitesimal profiles are independent of \tilde{A} .

The quasi-Newton iteration described in the previous section uses an error threshold of 10^{-9} , approximately the size of the floating point errors in approximating the

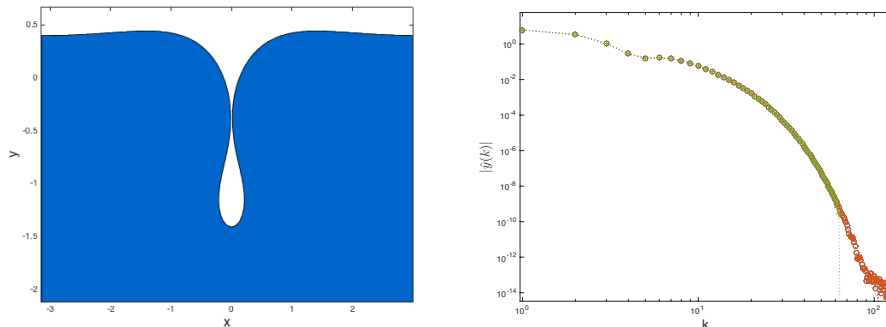


FIGURE 2. An example of a profile just before the self-intersecting configuration, for the branch of waves in Figure 1. The wave is depicted in the left panel. The right panel depicts the Fourier modes of the displacement, when $N = 128$ points, marked with green plus signs, and $N = 256$ points, marked with orange circles.

derivatives in the Jacobian matrix of the quasi-Newton iteration via finite difference approximations. The error is defined as the infinity norm of the Fourier modes of the projection of (12) and (17). The bulk of the numerical results use $N = 128$ points to discretize the interval of the pseudo-arclength $\alpha \in [0, 2\pi)$. When $N = 128$ the most extreme waves computed have Fourier modes which decay to approximately this threshold, thus the choice of our discretization and error threshold are self-consistent. As a check to see that the waves at this resolution are resolved to the reported threshold, we also computed a single, representative branch at $N = 256$. The waves profiles agree within the expected threshold; the Fourier modes of the extreme wave on this branch are reported at both resolutions are in the right panel of Figure 2. The profile used for this comparison is reported in the left panel of Figure 2.

From the perspective of the global bifurcation theorem, self-intersecting waves result in a branch terminating at finite amplitude, case (d) of the theorem. Standing waves signify a return to trivial, case (e) of the theorem. At a standing wave a branch of waves with positive speed is connected to a branch of traveling waves with negative speed. This setup can equally be interpreted as a branch which begins at one flat state configuration with one speed, and terminates at another flat configuration with a different speed.

We have numerically computed two examples of bifurcation surfaces, composed of a continuous family of branches of traveling waves with varying \tilde{A} . These bifurcations surfaces are presented in Figure 3. As extreme examples, we computed bifurcations surfaces with $A = 0$, the density-matched case, and $A = 1$ where the upper fluid is a vacuum. Each wave on these surfaces has the same values of $S = 0.25$ and $\tau = 2$. We present these surfaces in the three-dimensional space of c , \tilde{A} , and total displacement $h = \max(y) - \min(y)$. We chose to compute the surfaces for varying \tilde{A} , because the linear wave speeds don't depend on \tilde{A} . Thus the changes in the surface for different \tilde{A} are fundamentally due to large-amplitude, nonlinear effects. In both computed surfaces, ($A = 0$ and $A = 1$), we observe that for small \tilde{A} , branches of traveling waves terminate in self intersection. After some critical \tilde{A} , the

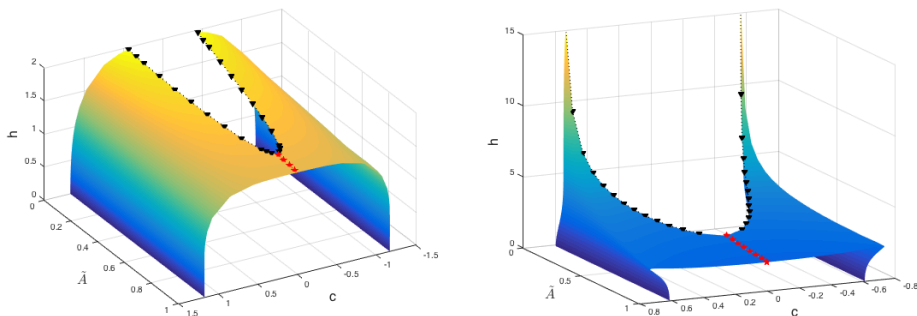


FIGURE 3. Two examples of bifurcation surfaces are depicted in the parameter space of \tilde{A} , c , and the total interface displacement $h = \max(y) - \min(y)$. These waves were computed with $S = 0.25$, $\tau = 2$ and $A = 1$ (left panel) and $A = 0$ (right panel). Branches with small \tilde{A} , in the back of the figure, terminate in self-intersecting waves, whose locations are marked with black triangles. In both cases, there is a critical \tilde{A} , corresponding to a switch from branches which terminate in self-intersecting waves to those which end in standing waves, whose locations are marked with red stars. The standing waves mark the merger of the surfaces of positive and negative speeds.

extreme wave on a branch is a standing wave; the branches of waves with positive speed are connected to branches of waves with negative speed, a “return-to-trivial” global bifurcation.

In addition to computing bounded branches of traveling waves, we observe evidence of an unbounded branch. In the case where the fluid densities match $A = 0$ and the interface has no mass $\tilde{A} = 0$, we found no evidence of a largest wave. Considering the limit as $\tilde{A} \rightarrow 0$, we observe a largest self intersecting wave with total displacement $h \sim \tilde{A}^{-1/2}$, suggesting that wave when $\tilde{A} \rightarrow 0$, the interfaces can be unboundedly large. This behavior is depicted both in the right panel of Figure 3 as well as in the left panel of Figure 4.

In search of an unbounded branch of traveling waves, we computed a branch of traveling waves in the configuration, $(\tilde{A}, A, S, \tau) = (0, 0, 0.25, 2)$. The results of this computation are in the center and right panels of figure 4. In the center panel are examples of increasingly large profiles of traveling waves. We observe no evidence of a largest profile, or any tendency toward self-intersection. The speed’s dependence on displacement is depicted in the right panel of Figure 4. The speed limits on a finite value, as the profiles become arbitrarily large. We consider this configuration an example of case (a) of the main theorem.

REFERENCES

- [1] M.J. Ablowitz and A.S. Fokas. *Complex Variables: Introduction and Applications*. Cambridge Texts Appl. Math. Cambridge University Press, Cambridge, 1997.
- [2] B. Akers, D.M. Ambrose, and J.D. Wright. Traveling waves from the arclength parameterization: Vortex sheets with surface tension. *Interfaces Free Bound.*, 15(3):359–380, 2013.
- [3] B. F. Akers and W. Gao. Wilton ripples in weakly nonlinear model equations. *Commun. Math. Sci.*, 10(3):1015–1024, 2012.

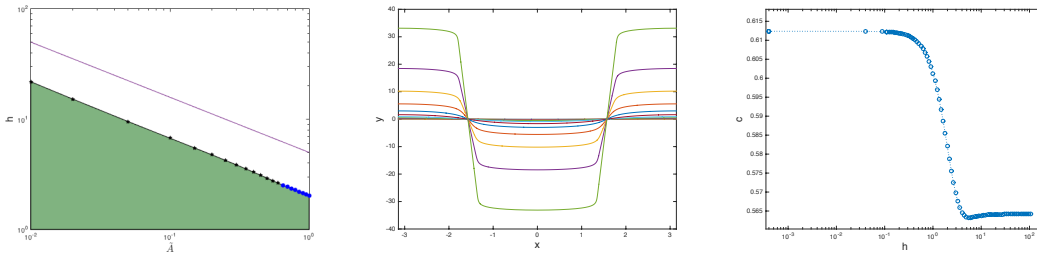


FIGURE 4. Numerical evidence of a branch of waves which contains interfaces of arbitrary length, case (a) of the main theorem. In the left panel, the displacement of the largest wave, h , for $A = 0, S = 0.25$, and $\tau = 2$, is depicted as a function of A . Numerical computations are marked, either self-intersecting waves or standing waves, using the marking convention of Figure 3. As a guide, the value $h = 5\tilde{A}^{-1/2}$ is marked with a solid line; waves exist in the shaded region. In the center are profiles computed at $(\tilde{A}, A, S, \tau) = (0, 0, 0.25, 2)$; no evidence of a largest profile was found. On the right is the speed amplitude curve, with a logarithmic horizontal axis, for the same configuration as the center. The speed limits on a finite value; thus, this is not case (f).

- [4] B.F. Akers, D.M. Ambrose, K. Pond, and J.D. Wright. Overturned internal capillary-gravity waves. *Eur. J. Mech. B Fluids*, 57:143–151, 2016.
- [5] B.F. Akers, D.M. Ambrose, and J.D. Wright. Gravity perturbed Crapper waves. *Proc. R. Soc. Lond. Ser. A Math. Phys. Eng. Sci.*, 470(2161):20130526, 14, 2014.
- [6] B.F. Akers and J.A. Reeger. Three-dimensional overturned traveling water waves. *Wave Motion*, 68:210–217, 2017.
- [7] S. Alben and M.J. Shelley. Flapping states of a flag in an inviscid fluid: bistability and the transition to chaos. *Phys. Rev. Lett.*, 100(7):074301, 2008.
- [8] D.M. Ambrose and M. Siegel. Well-posedness of two-dimensional hydroelastic waves. *Proc. Roy. Soc. Edinburgh Sect. A*, 2015. Accepted.
- [9] D.M. Ambrose, W.A. Strauss, and J.D. Wright. Global bifurcation theory for periodic traveling interfacial gravity-capillary waves. *Ann. Inst. H. Poincaré Anal. Non Linéaire*, 33(4):1081 – 1101, 2016.
- [10] P. Baldi and J.F. Toland. Bifurcation and secondary bifurcation of heavy periodic hydroelastic travelling waves. *Interfaces Free Bound.*, 12(1):1–22, 2010.
- [11] P. Baldi and J.F. Toland. Steady periodic water waves under nonlinear elastic membranes. *J. Reine Angew. Math.*, 652:67–112, 2011.
- [12] C.G. Broyden. A class of methods for solving nonlinear simultaneous equations. *Math. Comp.*, 19:577 – 593, 1965.
- [13] P. Guyenne and E.I. Părău. Computations of fully nonlinear hydroelastic solitary waves on deep water. *J. Fluid Mech.*, 713:307–329, 2012.
- [14] P. Guyenne and E.I. Părău. Finite-depth effects on solitary waves in a floating ice sheet. *J. Fluids Struct.*, 49:242 – 262, 2014.
- [15] H. Kielhöfer. *Bifurcation Theory: An Introduction with Applications to Partial Differential Equations*, volume 156. Springer, New York, 2 edition, 2012.
- [16] S. Liu and D.M. Ambrose. Well-posedness of two-dimensional hydroelastic waves with mass. *J. Differential Equations*, 262(9):4656 – 4699, 2017.
- [17] P.A. Milewski, J.-M. Vanden-Broeck, and Z. Wang. Hydroelastic solitary waves in deep water. *J. Fluid Mech.*, 679:628–640, 2011.
- [18] P.A. Milewski, J.-M. Vanden-Broeck, and Z. Wang. Steady dark solitary flexural gravity waves. *Proc. R. Soc. Lond. Ser. A Math. Phys. Eng. Sci.*, 469(2150):20120485, 8, 2013.
- [19] P.A. Milewski and Z. Wang. Three dimensional flexural-gravity waves. *Stud. Appl. Math.*, 131(2):135–148, 2013.

- [20] P.I. Plotnikov and J.F. Toland. Modelling nonlinear hydroelastic waves. *Philos. Trans. R. Soc. Lond. Ser. A Math. Phys. Eng. Sci.*, 369(1947):2942–2956, 2011.
- [21] P.H. Rabinowitz. Some global results for nonlinear eigenvalue problems. *J. Functional Analysis*, 7(3):487 – 513, 1971.
- [22] J. Reeder and M. Shinbrot. On Wilton ripples. I. Formal derivation of the phenomenon. *Wave Motion*, 3(2):115–135, 1981.
- [23] J. Reeder and M. Shinbrot. On Wilton ripples. II. Rigorous results. *Arch. Rational Mech. Anal.*, 77(4):321–347, 1981.
- [24] V.A. Squire, J.P. Dugan, P. Wadhams, P.J. Rottier, and A.K. Liu. Of ocean waves and sea ice. *Ann. Rev. of Fluid Mech.*, 27(1):115–168, 1995.
- [25] J.F. Toland. Heavy hydroelastic travelling waves. *Proc. R. Soc. Lond. Ser. A Math. Phys. Eng. Sci.*, 463(2085):2371–2397, 2007.
- [26] J.F. Toland. Steady periodic hydroelastic waves. *Arch. Ration. Mech. Anal.*, 189(2):325–362, 2008.
- [27] O. Trichtchenko, B. Deconinck, and J. Wilkening. The instability of wilton ripples. *Wave Motion*, 66:147–155, 2016.
- [28] Z. Wang, E.I. Părău, P.A. Milewski, and J.-M. Vanden-Broeck. Numerical study of interfacial solitary waves propagating under an elastic sheet. *Proc. R. Soc. Lond. Ser. A Math. Phys. Eng. Sci.*, 470(2168):20140111, 17, 2014.
- [29] Z. Wang, J.-M. Vanden-Broeck, and P.A. Milewski. Two-dimensional flexural-gravity waves of finite amplitude in deep water. *IMA J. Appl. Math.*, 78(4):750–761, 2013.
- [30] J.R. Wilton. LXXII. On ripples. *The London, Edinburgh, and Dublin Philosophical Magazine and Journal of Science*, 29(173):688–700, 1915.
- [31] Wolfram Research Inc. Mathematica 10.3 student edition, 2015.

DEPARTMENT OF MATHEMATICS AND STATISTICS, AIR FORCE INSTITUTE OF TECHNOLOGY, 2950 HOBSON WAY, WPAFB, OH 45433 USA

E-mail address: `benjamin.akers@afit.edu`

DEPARTMENT OF MATHEMATICS, DREXEL UNIVERSITY, 3141 CHESTNUT STREET, PHILADELPHIA, PA 19104 USA

E-mail address: `dma68@drexel.edu`

DEPARTMENT OF MATHEMATICS, DREXEL UNIVERSITY, 3141 CHESTNUT STREET, PHILADELPHIA, PA 19104 USA

E-mail address: `dws57@drexel.edu`